Weld Strength and Crack Growth Ductility from the Lazy-L Test

by

Chad Matthew Brooks

S.B. Mechanical Engineering
Massachusetts Institute of Technology
(1994)

Submitted to the Department of Mechanical Engineering
in Partial Fulfillment of the Requirements
for the Degree of

MASTER OF SCIENCE
IN MECHANICAL ENGINEERING

at the

MASSACHUSETTS INSTITUTE OF TECHNOLOGY

May 1995

Signature of Author Chad M. Brooks
Department of Mechanical Engineering
May, 1995

Certified by Frank A. McClintock
Professor Emeritus Frank A. McClintock
Thesis Supervisor

Accepted by
Professor Ain A. Sonin
Chairman, Graduate Committee

Weld Strength and Crack Growth Ductility from the Lazy-L Test

by

Chad Matthew Brooks

Submitted to the Department of Mechanical Engineering on May 12, 1995, in partial fulfillment of the requirements for the degree of Master of Science in Mechanical Engineering.

Abstract

Fully plastic fracture of fillet welded T-joints is characterized by the limit moment, slip line displacement to crack initiation, and crack growth ductility, defined as the slip line displacement per unit crack advance. A novel fillet weld fracture experiment, the Lazy-L Test, is developed as a simple, inexpensive method of measuring data used to calculate these parameters. Fully plastic fracture mechanics provides an extrapolation of Lazy-L Test results to other fillet weld failure modes observed in ship grounding, including peeling of the shell plating. The Lazy-L Test is introduced as an alternative to more costly and difficult experimental and computer methods, and suggested for consideration as a standard test in the design and qualification of fillet welds for service.

The Lazy-L is used to test single fillets in predominant bending (opening from the root of the weld), single fillets in predominant transverse shear, and double fillets in predominant bending. The plastic flow field for each configuration is modeled by single arcs of sliding in the fillet selected to yield a least upper bound to the limit moment. Load-displacement data for each configuration determine an experimental limit moment, displacement to initiation and crack growth per unit slip line displacement. The results are generalized for other weld loadings when expressed in terms of the mean normal stress across the crack tip.

Twelve experiments are presented for 6mm and 9mm weld sizes produced using GMAW with the combination of LR-EH36 steel plate and E7016 stick electrode. With the modeling assumptions of plane strain, homogenous weld metal shear strength and small angles of deformation, the experimental limit moments for single fillet shear and double fillet bending range from 10-20% above predicted values. Single fillet bending limit moments vary more significantly, and lead to the selection of alternate models including an edge-notched bar of weld metal in bending. Displacements to crack initiation are consistent throughout the data sets and experimental crack growth ductility rates are within 10-20% of the predicted values from prior stutudies of overmatched welds.

These results encourage further study of the Lazy-L Test configuration to establish an experimental database over a range of material, geometry, and welding process parameters.

Thesis Supervisor: Frank A. McClintock
Title: Professor Emeritus, Mechanical Engineering

Acknowledgments

This research was sponsored by members of the Joint M.I.T - Industry Project for Tanker Safety, Professor T. Wierzbicki, Principal Investigator. Testing facilities were provided by the M.I.T. Lab for Manufacturing and Productivity, and the Mechanical Behavior of Materials Lab, Department of Mechanical Engineering. Welding was performed by Atomic Ltd., Cambridge, Massachusetts. Machining was provided by the M.I.T. Lab for Nuclear Science Machine Shop.

I thank Professor Wierzbicki for his enthusiastic leadership of the tanker safety project and Professor K. Masubuchi for his guidance and support of the welding and fabrication team. I also thank team members R. Wilcox, J. Atmadja, and R. Middaugh for their valued contributions and encouragement.

Finally, I gratefully thank Professor F.A. McClintock for his tireless devotion and patience as a teacher and supervisor. His insight, professionalism, and passion for engineering have been inspiring.

Table of Contents

List of Figures

List of Tables

List of Symbols

α	included angle of Lazy-L specimen Leg A and the test surface
β	included angle of Lazy-L specimen Leb B and the test surface
δ_{vert}	vertical displacement due to specimen compliance
μ	coefficient of friction
$\phi_A, \phi_B, \phi_C, \phi_D$	slip arc angles
σ_A, σ_C	mean normal stress across the slip line at the fillet root
σ_y	yield strength
θ	relative rotational displacement of Lazy-L specimen legs
a	crack length
b	ligament width
C_{dr}	displacement-rotation conversion factor
C_{lm}	load-moment conversion factor
d	weld leg length
D	diameter of 3/4-round support
D_g, du_s/da	crack growth ductility factor (inverse of crack growth rate per unit slip line displacement)
E	Young's modulus
h_a,	effective height rise of specimen leg due to relative rotation
I	moment of inertia
k_f	fillet weld shear strength
k_w	web metal shear strength
L_a	length of Lazy-L specimen Leg A
L_b	length of Lazy-L specimen Leg B
M	moment per unit weld length
$(M_{norm})_{web}$	normalizing moment of web.
$(M_{norm})_{weld}$	normalizing moment of bar of fillet weld metal
M_{tot}	total weld moment
N_a, N_b	moment arm of Lazy-L specimen leg reaction forces
P	applied load
r_a, r_c	slip arc radii
R_a, R_b	Lazy-L specimen leg reaction forces
R_{weld}	tear resistance
t_w	web metal thickness
u_s	slip line displacement
$(u_s)_{init}$	slip line displacement to crack initiaiton
dv/dP	compliance
v_m	measured displacement of Lazy-L specimen
w	weld length

1 Introduction

Renewed consideration of the crash worthiness of oil tankers has demonstrated the need for more detailed characterization of hull fillet weld failure due to grounding loads. (Wierzbicki, et al, 1991) Existing fillet weld design standards have been formulated to ensure safe performance under normal operating conditions but do not guarantee fillet weld integrity under extreme loading conditions. The next generation of fillet weld standards must specify fillet weld parameters of interest for crash worthiness analyses and provide simple, flexible tests for measuring those parameters over a range fillet weld design choices.

This paper introduces a simple test, named the "Lazy-L" for its appearance, which provides data to quantify fillet weld failure parameters which may be extrapolated to the peeling mechanism observed at the interface of the stiffeners and shell plating. These parameters are the limit moment of the weld, the displacement to crack initiation, and the crack growth ductility factor expressed as the inverse of the crack growth rate per unit slip line displacement. These parameters characterize both the initial plastic sliding and subsequent ductile fracture observed in the peeling failure mechanism. They also allow computation of the tearing work per unit weld length for use in structural analyses of hull grounding. (McDonald, 1994) The Lazy-L configuration is shown as Fig. 1.

1.1 Background

Public awareness of oil tanker crash worthiness was heightened by the 11 million tons of spillage resulting from the March 1989 grounding of *Exxon Valdez* in Prince William Sound, Alaska. Congress responded to the incident with passage of the Oil Pollution Act of 1990 (OPA90) which mandates that all U.S. and foreign flag vessels operating in U.S. waters and constructed or overhauled after June 30, 1990 must have a

double hull. The Secretary of Transportation, directed to establish the requirements of a double hull, is authorized to propose to Congress alternative methods which provide the same level of environmental protection as a double hull. (Federal Register, Vol. 55, No. 234)

In the interest of satisfying the mandate of OPA90 as well as protecting the environment and valuable cargo, the M.I.T. "Joint Industry Project on Grounding Protection of Tankers" formed in September 1992 to develop technology for assessing, designing, and certifying spill resistant tankers. Specifically, the project was directed towards predicting structural damage in grounding, providing improved design and fabrication methods to resist grounding, and developing performance standards for tankers.

1.2 Objectives

In view of these goals, a welding a fabrication team was established within the M.I.T. Tanker Safety Project to conduct an analytical and experimental study of the strength of fillet welds. Specific tasks included an experimental study of the tearing strength of T-joints subjected to bending, peeling, or tension, and an analytical study of the bending and tensile strengths of fillet welds using simple plastic fracture mechanics. This study addresses these tasks by providing an application of previously developed fully plastic fracture mechanics for welded T-joints (McClintock, 1994) in the development of a novel experimental configuration which provides data to quantify limit moment, displacement to crack initiation, and the crack growth ductility. This is achieved by using plastic slip line models to provide equations for design and data analysis, leading to weld limit moment, slip line displacement to initiation, crack growth ductility, and predictions of the critical peeling work. Further, such data are provided from a pilot study.

The proposed test configuration is intended as a tool for designers and fabricators of fillet welded T-joints. The test is flexible in that three different experiments are available from the same general setup. The first is a single fillet in the upper position of Fig. 1 which experiences predominant bending. The second is a single fillet in the lower position which experiences predominant transverse shear and fails in a plastic fracture similar to that for pure tension. The third is a double fillet bending experiment which simulates web folding. Throughout the development of the test, an effort has been made to maintain the simplicity of specimen design, experimentation, and data analysis. With further experimentation and development, it is proposed that the Lazy-L configuration be adopted as an industry standard for the design and qualification of fillet welds for service.

1.3 Paper Organization

The paper provides an introduction to the Lazy-L test and related analysis at several levels of detail. Chapter 2 provides an overview of essential specimen design and data interpretation methods with only the relevant results of the theoretical development. A more detailed treatment begins with Chapter 3 which elaborates the plastic slip line theory for fillet welds. Chapter 4 presents complete specimen and fixture design relations for the range of experiments possible with the Lazy-L test. Chapter 5 outlines specific steps in the design and fabrication of test specimens and fixtures. Chapter 6 details data analysis and interpretation methods. Chapter 7 provides the specifications, results and interpretation of a pilot study of the Lazy-L test configuration. Chapter 8 provides conclusions and recommendations. The Appendices, referenced from the body of the report, present computer methods and procedural notes helpful in conducting tests. Figures and tables referenced in the body of the report are included after Chapter 8. Figures and tables for the Appendices are provided at the end of the Appendix in which they are referenced.

2 Overview of the Lazy-L Test

2.1 Introduction

Existing fillet weld standards, such as the American Bureau of Shipping tack welder qualification test No. 3 shown as Fig. 2, test for qualitative weld characteristics associated with fabrication including porosity, uniformity and undercut.(ABS, 1991) To predict fillet integrity under grounding loads, more quantifiable measures are needed. In bending, these parameters include the limit moment, rotation to crack initiation and load drop per unit bend angle. In tension, these are the tear resistance, limit load, and load drop per unit extension across the weld. Fracture mechanics for plastic slip lines demonstrate that these quantities may be expressed as functions of weld hardness, slip line displacement to initiation as a function of the normal stress across it, and crack growth rate per unit slip as a function of the mean normal stress across the crack tip. (McClintock, 1994)

The Lazy-L test is an inexpensive, versatile experiment which provides data to calculate limit moment, displacement to initiation and crack growth ductility, defined as slip line displacement per unit crack advance. The plastic flow field is modeled as a single arc of sliding in the weld chosen to yield the least upper bound to the limit moment. The results may be applied to designing fillet welds against peeling, tension and combined loading.

2.2 Lazy-L Test Configurations

The Lazy-L Test specimen is a modified 90° lap joint in which enough overhang is allowed to accommodate a 45° fillet. The specimen is loaded in compression to

produce a bending moment at the weld. Load-displacement data and specimen geometry are used to calculate the moment-rotational displacement characteristic of the specimen.

As demonstrated in Fig. 1, three joint configurations are available in the Lazy-L test. The first is a single fillet in the upper position which is subjected to predominant bending. The second is a single fillet in the lower position which is subjected to predominant transverse shear. The fracture for this configuration is very similar to that observed in pure tension and indicates the feasibility of extrapolating strength and crack initiation results to fillet welds in tension. The third configuration is a double fillet in bending which simulates web folding.

The plastic flow field for each configuration is represented as an arc of sliding. The arc is chosen which results in a least upper bound to the limit moment. The limit moments govern specimen sizing to assure weld failure. Constraints include sufficient width for plane strain, low machine and specimen compliances for stable fracture, small plastic deformation of the web, and low friction at contact points between the specimen and support fixtures.

2.3 Specimen and Fixture Design for Weld Failure

The Lazy-L specimen is designed for a particular combination of web metal, filler metal, and welding process of interest. These choices fix the weld leg length, d, web metal shear strength, k_w, and fillet metal shear strength, k_f. These parameters are assumed constant throughout the design process. Fow weld failure, the web thickness, t_w, may need to be increased to prevent leg yielding or to reduce complaince. The following design steps have been simplified by the assumption of negligible friction and specimen symmetry.

Step 1: Weld length. For a given weld configuration, choose weld length, w (equal to specimen width), of ten times the weld leg to satisfy plane strain. Longer welds require proportionately larger machine capacity.

Step 2: Web thickness. Taking the moment of a bar of fillet metal as the normalizing variable for a single fillet in bending, the minimum normalized limit moment is 1.475 for all combinations of web thickness and weld leg length. The least upper bound to the limit moment of the weld is:

$$M = (\frac{M}{M_{norm}})M_{norm} = 1.475 k_f d^2 / 2 \qquad (2.1)$$

Normalized bending moments for single fillet shear and double fillet bending are more complicated functions of the ratio of web thickness to weld leg length, t_W/d, and the ratio of weld shear strength to web shear strength, k_f/k_W. When the normalizing variable is taken as the moment of the web, the relationships are as shown in Fig. 3 and Fig. 4. The least upper bound to the limit moment of the weld, M, is the product of the minimum normalized bending moment from the appropriate graph and the nominal bending moment of the base metal:

$$M = (\frac{M}{M_{norm}})k_w t_w^2 / 2 \qquad (2.2)$$

Choose web thickness so that the moment for specimen leg yielding is greater than the weld moment.

Step 3: Specimen Leg Length. The specimen leg length is chosen for sufficient stiffness and to achieve the limit moment of the weld, M, for a load safely within machine capacity. First, reaction forces at contact points are expressed as functions of the applied load, P, by applying equilibrium conditions to the specimen. Next, the specimen is divided at the weld into two free bodies for which the equilibrium conditions can be solved for weld moment in terms of applied load. For a symmetric specimen with negligible friction and small sliding arc radii compared tc specimen leg length, a load-moment relation for the Lazy-L specimen may be expressed as:

$$M = \frac{P\sqrt{2}}{4}(L - t_w) \tag{2.3}$$

where L is the specimen leg length measured from the joint. Choose L to achieve the weld moment for the available load capacity.

At this stage of design, the specimen geometry is fully specified. The remaining steps predict specimen behavior during testing and suggest design changes for improved performance.

Step 4: Specimen Leg Yielding. The first consideration is plastic deformation of the specimen leg. With the assumption of small web thickness compared to specimen leg length, plastic deformation occurs in the base material when:

$$\sigma_y < \frac{6M}{w{t_w}^2} \tag{2.4}$$

where σ_y is the yield stress of the web metal. Web metal thickness may be increased to prevent yielding; however, the normalized limit moment and the peak load also increase.

Step 5: Specimen Compliance. The final consideration for specimen design is crack growth stability. Stable crack growth occurs only when the steepest load drop per unit deflection is larger than the sum of machine and specimen compliances. This displacement must be estimated for the particular weld, but is in the range of 0.7-1.0 degrees of rotation from prior work on crack growth ductility factor. (Lyman, 1969) The estimated rotation is related to measured displacement by specimen geometry. In the symmetric specimen, this relation is:

$$v_m = \frac{L}{2\sqrt{2}}\theta \tag{2.5}$$

where v_m is measured displacement and θ is rotation at the joint.

Machine compliance is often provided but varies with the test direction. In displacement machines, it may be measured by compressing an aluminum cylinder and subtracting the cylinder compliance from the measured data. Specimen compliance is found by applying beam bending equations to the specimen legs. For the symmetric specimen, measured displacement is related to the applied load by:

$$v_m = \frac{PL^3}{Ewt_w^3} \tag{2.6}$$

where E is modulus of elasticity of the web metal. Specimen compliance is reduced by increasing base metal thickness and reducing specimen leg length; however, these changes increase the peak load. If the test is not stable for a specimen requiring nearly the entire machine capacity, a larger, more rigid machine must be used for testing.

The test fixtures are the same for all Lazy-L specimen configurations. Three steel 3/4-round cylinders of length w reduce friction to negligible levels when well-lubricated with oil, grease or Teflon spray. The specimen is supported by a hardened steel plate and is compressed using a flat plate grip. Steel for the 3/4 rounds and plates are chosen to prevent local yielding at the contact points as predicted in Roark. (see Chapter 5) Shielding is required during testing to prevent projectiles in the event of unstable fracture.

2.4 Data Analysis and Interpretation

Characteristic load-displacement data for the Lazy-L experiment include an elastic loading region followed by a region of plastic deformation and subsequent load drop due to crack initiation and propagation. The similarity of the data reduction relations and experimental design relations facilitate data processing and suggest the use of spreadsheets for both operations. First, an experimental normalized bending moment is obtained by entering the peak measured load into Equation (2.3) and dividing by the moment of the web metal. The measured displacement at crack initiation, indicated by the beginning of a steep load drop, is equated to a rotational displacement according to Equation (2.5). This rotation is related to displacement along the arc of maximum shear in the weld by the radius of the arc presented for representative specimens in Table 1. Finally, displacement along the arc of sliding per unit crack advance is computed by relating the moment change associated with an incremental displacement along the slip line with a reduction of weld ligament due to crack growth.

Application of these values to other loading conditions is described in Chapter 6.

2.5 Conclusion

The Lazy-L test shows promise as a practical, simple and inexpensive means of measuring critical fillet weld parameters for use in gauging overall joint integrity. These paramters may be used in comparative studies to measure the effectiveness of changes to fillet weld design.

3 Plasticity for the Lazy-L Test

3.1 Introduction

Fillet welded T-joints are difficult to analyze due to complex geometry. Further, material properties in the fillet, web metal and heat affected zone, which are a function of both the original material properties and the welding process parameters, are not homogeneous. For these reasons, previous analyses of fillet weld performance under critical loading conditions have utilized equilibrium across a single section such as the fillet throat or fillet-web interface which, except for longitudinal shear, produce neither exact solutions nor bounds to it. The following summarizes an application of fully plastic fracture mechanics for fillet welded T-joints, developed by McClintock, to compute a least upper bound to the limit moment of the weld.

The steels used in ship hull construction are ductile enough that the plastic deformation observed in collisions and groundings is large compared to the elastic deformation. Further, at the limit load, elastic strain increments are zero.(McClintock, Kim, Parks 1993) Additionally, non-hardening, rate-independent plasticity is presented as a practical limiting case. Throughout the development, the plane strain approximation is used.

3.2 Bounds to the Limit Moment from Plastic Slip Line Fields

The moment in a moment-displacement curve of a plastic member rises steeply in the elastic region and is virtually constant in the plastic region before dropping off due to thinning or fracture. The nearly constant moment is called the limit moment and is a measure of the strength of the member for the given loading. An exact solution for the limit moment or the limit load of a member is difficult to calculate, even without strain

hardening, since it must satisfy no less than five conditions of mechanics: (i) the partial differential equations of equilibrium of stress gradients, (ii) the definitions of components of strain in terms of displacement gradients, (iii) boundary conditions in terms of displacements or tractions, (iv) a yield locus which limits the magnitudes of the stress components, and (v) linear functions relating the increments of strain components to the current stress components. Exact solutions to the limit moment for plane strain and strain-hardening are best expressed in terms of possibly curved lines parallel to the two directions of maximum shear stress at a point. (McClintock, 1994) These lines together form a slip line field. Constructing complete slip line fields involves discovering a field that satisfies (a) the Hencky equations for equilibrium and yield condition in the deforming region, (b) the Geiringer equations for incompressibility in the deforming region, and (c) equilibrium and the yield inequality in the rigid region.(Kim, McClintock, Parks, 1993) Although slip line fields have been developed for a number of common geometries (e.g. Chakrabarty, 1987), developing a slip-line field for a novel geometry is a matter of experience, insight and possibly experimentation.

Fortunately, an upper bound to the limit moment is found from the plastic work of incompressible displacement fields which satisfy any displacement boundary conditions. (e.g. McClintock, 1994) Useful upper bounds to the limit moment can be constructed from kinematically admissible deformation fields consisting of circular arcs of sliding. Upper bounds found in this way often provide estimates within 20% of the limit moment. (McClintock, 1994) Kim, McClintock and Parks demonstrate that if stresses on the arc which yields the least upper bound, called the LUB arc, are chosen to satisfy one global equilibrium condition, they satisfy all conditions (a)-(c) above. (Kim, McClintock, Parks, 1993) Lower bounds are rarely practical due to the difficulty of satisfying the equilibrium equations and yield criterion everywhere, even in the rigid region.

3.3 Upper Bounds to the Limit Moment in the Lazy-L Test

As shown in Fig. 5, a hardness survey of a fillet weld has revealed that the hardness within the weld is roughly uniform and is less than that of the surrounding heat affected zone.(Middaugh, 1994) As a first estimate, therefore, the plastic flow fields for the fillet welds and surrounding web metal are modeled as arcs of maximum shear through the weld metal. The arcs separate the structure into two sections with the lower section remaining fixed while the upper section rotates about the focus of the arcs. The product of this rotation and the applied moment is equal to the work done in sliding along the arcs against the shear strength of the weld metal, k_f.

The arc focus is adjusted until the arcs of sliding produce the minimum limit moment. As will be illustrated, the limit moment of the single fillet in bending is not a function of the web metal properties and is normalized by the moment of a bar of weld metal. In the cases of a single fillet in transverse shear and double fillet in bending, the normalizing variable is the moment of a bar of web metal. Iterative minimization methods, described in Appendix 1, are performed using Microsoft Excel spreadsheets.

The following analyses utilize the shear strength of the fillet and web, k_f and k_w, respectively. Means of estimating these values from Rockwell superficial hardness readings and corresponding tensile strengths are presented in Appendix 3. Note that the shear strength of the web metal, k_w, is calculated as the tensile strength divided by $\sqrt{3}$; however, prior studies conclude that shear strength of the fillet weld metal, k_f, is better approximated as the tensile strength times 0.75. (Krumpen and Jordan, 1984)

3.3.1 Bound for Single Fillet in Predominant Bending

Calculation of an upper bound to the limit moment for the single fillet bending configuration begins with the selection of an arbitrary arc of sliding through the fillet as

shown in Fig. 6. The arc is characterized by a radius of curvature, denoted by r_c in the figure, and angles ϕ_C and ϕ_D measured from a tangent to the arc of sliding clockwise to the face of the weld. Note that angle ϕ_C is a constant 135°. The moment, M, times a rotation $\delta\theta$ is equal to the work done in sliding along the arc of radius r_c against the shear strength of the fillet weld metal, k_f, and may be expressed in term of the angle difference $(\phi_C - \phi_D)$ in radians:

$$M\delta\theta = k_f[r_c(\phi_C - \phi_D)]r_c\delta\theta \tag{3.1}$$

The angles and the radius of curvature are related to the weld leg, d, by expressing the weld throat, $d/\sqrt{2}$, as the sum of two line segments, shown as solid lines through the weld in Fig. 6, which may in turn be expressed as functions of r_c and the angle ϕ_D by the following relation:

$$\frac{d}{\sqrt{2}} = r_c \sin 45^\circ + r_c \sin(90^\circ - \phi_D) \tag{3.2}$$

The angle ϕ_D is now expressed in terms of the arc of curvature, r_c and the weld leg length, d, by solving (3.2) for ϕ_D:

$$\sin(\pi/2 - \phi_D) = \cos(\phi_D) = \frac{d}{r_c\sqrt{2}} - \frac{1}{\sqrt{2}} \tag{3.3}$$

The normalizing moment in the single fillet opening case is the moment of a bar of fillet weld metal of throat thickness, $d/\sqrt{2}$:

$$(M_{norm})_{weld} = \frac{2k_f(\frac{d}{\sqrt{2}})^2}{4} = \frac{k_f d^2}{4} \tag{3.4}$$

The non-dimensionalized expression of M/M_{norm}, per unit weld length, is constructed by dividing Equation (3.1) by Equation (3.4):

$$M / M_{norm} = 4(\frac{R_c}{d})^2(\phi_C - \phi_D) \tag{3.5}$$

For chosen values of weld leg length, d, the value of r_c is chosen which, for $\phi_C = \pi/2$ and ϕ_D from Equation (3.3), minimizes M/M_{norm}. Minimization methods are described in Appendix 1 and summarized in Table 1. Note that the minimum value of M/M_{norm} is the same for all single fillets in predominant bending since it is a function only of weld leg length with which the arcs of sliding scale.

3.3.2 Bound for Single Fillet in Predominant Transverse Shear

The minimum normalized bending moment for the single fillet in predominant transverse shear is a function of the web thickness, t_w, as well as weld leg, d. Also, both angles are functions of the radius of curvature, r_a. Figure (7) illustrates the geometry for the single fillet in transverse shear. As before, the first step is to assume an arbitrary arc of sliding through the weld which is now characterized by the radius of curvature, ra. Other variables include the height of the center of rotation, h, and the point of intersection of the arc and the free surface of the weld, denoted by (x,y) coordinates with respect to the reference axes shown in the figure.

The moment, M, times a rotation $\delta\theta$ is equal to the work done in sliding along the arc of radius r_a against the shear strength of the fillet weld metal, k_f, and may be expressed in term of the angle difference $(\phi_B - \phi_A)$ in radians:

$$M\delta\theta = k_f[r_a(\phi_B - \phi_A)]r_a\delta\theta \tag{3.6}$$

The angles ϕ_A and ϕ_B may be expressed in terms of the web thickness, and variables h, x, y, and r_a:

$$\phi_A = [\frac{\pi}{2} - \cos^{-1}(\frac{t_w}{r_a})] = \cos^{-1}(\frac{h}{r_a}) \tag{3.7}$$

$$\phi_B = [\frac{\pi}{2} + \cos^{-1}(\frac{y-h}{r_a})] = \cos^{-1}(\frac{h-y}{r_a}) \tag{3.8}$$

The assumption of 45° welds results in the relation x = y for any arc. The complete set of relations for x, y, h, and r_a are summarized as:

$$\begin{aligned} x &= y \\ r_a^2 &= h^2 + t_w^2 \\ r_a^2 &= (y-h)^2 + (t_w + d - x)^2 \end{aligned} \tag{3.9}$$

Given a web thickness, t_w, and a weld leg length, d, Equations (3.9) are solved simultaneously for assumed values of the height of the center of rotation, h. Upon substitution, Equations (3.8) reduce to a quadratic relation solvable for the x and y coordinate in terms of height, h, leg length, d, and web thickness, t_w:

$$x = \frac{h + (t_w + d) - \sqrt{h^2 + 2h(t_w + d) - (t_w + d)^2 + 2{t_w}^2}}{2} \tag{3.10}$$

For various h, the arc radius, r_a, and the angles ϕ_A and ϕ_B are computed directly from Equations (3.7)-(3.9). For single fillet shear, the normalizing moment is chosen as the moment of a bar of web metal of thickness, t_W:

$$(M_{norm})_{web} = \frac{2k_w{t_w}^2}{4} = \frac{k_w{t_w}^2}{2} \tag{3.11}$$

where k_W is the shear strength of the web metal. The non-dimensionalized moment M/M_{norm}, per unit weld length, is constructed by dividing Equation (3.6) by Equation (3.11):

$$M / M_{norm} = \frac{2k_f{r_a}^2(\phi_B - \phi_A)}{k_w{t_w}^2} \tag{3.12}$$

The minimization of Equation (3.12) requires iterative selection of the height of the center of rotation, h, solution of the radius of curvature, r_a, and the coordinates, (x,y), and solving for the angles, $(\phi_B - \phi_A)$. This procedure is suitable for spreadsheet solutions such as those presented in Appendix 1. Results for the test specimens described in Chapter 6 are presented in Table 1. Because of the dependence of M/Mnorm on web thickness and material shear strengths, each specimen has a unique minimum normalized moment.

3.3.3 Bound for Double Fillet in Predominant Bending

The minimum normalized bending moment for a double fillet in bending is an extension of the single fillet in predominant transverse shear to include the influence of the additional fillet. The geometry, illustrated in Figure (8), requires that the height of the center of rotation of the arc of sliding for the fillet in transverse shear, h, equal the radius of curvature for the fillet in bending, R_c. Therefore, the analysis for the single fillet in transverse shear is used to determine radii of curvature, r_a and r_c, for the two arcs of sliding.

The moment, M, times a rotation, $\delta\theta$, is equal to the work done in sliding along arcs of radii r_a and r_c against the shear strength of the fillet weld metal, k_f, and may be expressed as:

$$M\delta\theta = k_f\{[r_c(\phi_C - \phi_D)]r_c + [r_a(\phi_B - \phi_A)]r_a\}\delta\theta \qquad (3.13)$$

Notice from Figure (8) that the angles ϕ_C and ϕ_D are now measured counter clockwise from the tangent to the arc of sliding to the horizontal. As a result, $\phi_C = 0$ and ϕ_D is:

$$\phi_D = 135^\circ - \cos^{-1}\left(\frac{d}{r_c\sqrt{2}} - \frac{1}{\sqrt{2}}\right) \qquad (3.14)$$

When the normalizing moment is taken as that for a bar of web metal of thickness t_w, the normalized bending moment for the double fillet in bending is constructed by dividing Equation (3.13) by Equation (3.11):

$$M / M_{norm} = \frac{2k_f[r_c^2(\phi_C - \phi_D) + r_a^2(\phi_B - \phi_A)]}{k_w t_w^2} \tag{3.15}$$

Minimization methods for Equation (3.15) is presented in Appendix 1 with key results for the test specimens of Chapter 6 summarized in Table 1.

4 Relations for Specimen Design and Data Reduction

4.1 Reaction Forces from Applied Load and Geometry

The Lazy-L configuration is analyzed using simple trigonometric and mechanical equilibrium relations. In this section, reaction forces on the legs are developed as functions of geometry and applied load. These forces are later used to calculate the bending moment at the weld.

The legs of the Lazy-L specimen are assumed to be joined at right angles as shown in Fig. 9. L_a and L_b represent the overall dimension of the specimen legs while L_b represents the length of leg B below the intersection of the two members.

The interior angles of the triangle formed by the Lazy-L specimen, noted as α and β in Fig. 9, are:

$$\alpha = \tan^{-1}\left(\frac{L_b - 2t_w}{L_a}\right) \tag{4.1}$$

$$\beta = \frac{\pi}{2} - \alpha \tag{4.2}$$

These angles are used to compute moment arms of the reaction forces with respect to the point at which the load, P, is applied. Since the load, P, and the reaction force, R_b, are applied to opposite corners of Leg B, the moment arm of R_b must be a function of both the length, L_b, and thickness, t_w, of Leg B. As shown in Fig. 10, this relationship is developed by imagining an extension of the outside edge of member B, which intersects the horizontal at angle β. The moment arm of reaction force R_b is equal to the moment arm of an imagined reaction for the extended leg less the horizontal component, x. The moment arm of the reaction force R_a is the horizontal span of the Lazy-L specimen less the moment arm of reaction force R_b:

$$N_b = (L_b + \frac{t_w}{\tan\beta})\cos\beta - \frac{t_w}{\sin\beta} \tag{4.3}$$

$$N_a = \frac{m}{\cos\beta} - N_b \tag{4.4}$$

A moment balance about the point of load application and a force balance for the specimen are solved simultaneously for R_a and R_b as functions of the applied load:

$$P = R_a + R_b \tag{4.5}$$

$$R_a N_a = R_a N_b \tag{4.6}$$

These relations are entered into spreadsheet to produce output such as Table 2. The expressions of R_a and R_b as functions of P are now used with appropriate diagrams of the separated Lazy-L specimens to arrive at an expression of the joint moment as a function of applied load.

4.2 Weld Moment from Reaction Forces

An experimental, non-dimensionalized limit moment is a useful output of the Lazy-L Test. The weld moment is expressed in terms of the measured load and specimen geometry. Such relations are derived for each of the three test configurations using appropriately selected free body diagrams and equilibrium equations. In each case, the moment is expressed in terms of a reaction force which is in turn a function of load and geometry; therefore, the moment may be expressed as the product of the applied load and a load-moment conversion factor, C_{lm}. Such conversion factors are computed for the specimens of the pilot study and presented in Table 2.

Single Fillet in Predominant Transverse Shear

Fig. 11 depicts the diagrams used to develop a relationship between the measured load and the weld moment, M_W, for the weld in predominant shear and tension. Body A is taken as Leg A of the Lazy-L specimen while Body B is taken as Leg B and all of the weld metal. Globally external forces include the applied load, reaction forces, and friction forces, $\mu_X R_{X_a}$ acting at the points of contact between the legs and test bed. Several internal forces are considered including a friction and contact force, μN and N, acting between the specimen legs, and a moment, shear, and contact force, M_W, S, and W, acting between Leg A and the weld metal.

Assuming pure bending of specimen leg (valid for long speimen legs), a relationship between P and the resultant moment of the internal forces arises from a solution of the moment equilibrium relations for either of the bodies. The moment equilibrium relations for Body A is:

$$\Sigma M_{x'} = 0: R_a(L_a - r_c)\cos\alpha - N(T_w) - \mu_a R_a(L_a - r_c)\sin\alpha - M_w = 0 \qquad (4.7)$$

This relations reduce to the following expression for the resultant weld moment, M_W:

$$M_w = R_a(L_a - r_c)\cos\alpha - \mu_a R_a(L_a - r_c)\sin\alpha - R_a t_w(\sin\alpha + \mu_a\cos\alpha) \qquad (4.8)$$

where L_a, t_W and α are geometrical parameters of the Lazy-L specimen, r_c is the radius of the least upper bound arc, and μ_a is the coefficient of friction between Leg A of the specimen and the test bed. As illustrated in section 4.1, the reaction force, R_a, is expressed in terms of the applied load, P.

Single Fillet in Predominant Bending

Fig. 12 illustrates the free body diagrams used to establish a relation between applied load, P, and weld moment, M_W, for a single fillet in predominant bending. The weld is split along the throat into two equal segments. Body A is taken as Leg A of the specimen along with half of the weld metal while Body B is Leg B along with the remaining weld metal. External forces include the applied load, reaction forces, and friction forces acting at the points of contact between the legs and test bed. The moment at the weld, M_W, becomes external to the bodies. Additional forces required to satisfy static equilibrium of Body A, a shear and contact force, act at the point of rotation between the two bodies and do not enter the moment balance. A relationship between applied load and weld moment can be derived from a single equation:

$$R_a[(L_a - r_c)\cos\alpha - t_w \sin\alpha] - \mu_a R_a[(L_a - r_c)\sin\alpha + t_w \cos\alpha] - M_w = 0 \qquad (4.9)$$

where L_a, t_W and α are geometrical parameters of the Lazy-L specimen, r_c is the radius of the least upper bound arc, and μ_a is the coefficient of friction between Leg A of the specimen and the test bed. Rearranging to solve for M_W:

$$M_w = R_a(L_a - r_c)\cos\alpha - \mu_a R_a(L_a - r_c)\sin\alpha - R_a t_w(\sin\alpha + \mu_a \cos\alpha) \qquad (4.10)$$

This result indicates that despite the change of geometry from the single fillet in transverse shear to the single fillet in predominant bending, the load-moment relation remains unchanged when the center of rotation is chosen as the focus of the arc of maximum shear.

Double Fillet in Predominant Bending

Separation of a double fillet specimen into free bodies requires the introduction of reaction forces which act at each weld. The result is that each free body is statically indeterminate; however, when the center of rotation is again chosen as the focus of the arc of maximum shear, the load-moment relation for double fillet bending is the same as for single fillet bending, Equation (4.10).

4.3 Weld Rotation from Measured Displacement

In order to interpret displacement data, we must relate the measured displacement, v_m, to the relative rotations, θ, between the two specimen legs. This relative rotation is later related to displacement along the arc of sliding through the weld, du_s. The displacement-rotation relation is developed for the case in which the Lazy-L specimen legs remain rigid throughout the test.

Fix Leg B of the specimen and impose a displacement vector perpendicular to Leg A as shown in Fig. 13. Assuming small angles, the height rise at A, h_a, is expressed as:

$$h_a = L_a \theta \cos\alpha \tag{4.11}$$

The height rise results in a rigid body rotation, $d\gamma$, about point B. Again assuming small angles:

$$L_a d\theta \cos\alpha = (\overline{AB}) d\gamma \tag{4.12}$$

where the segment, $\overline{AB}$, is the span of the Lazy-L specimen defined as:

$$(\overline{AB}) = L_a \cos\alpha + m\cos\beta \tag{4.13}$$

where m is the length of Leg B below the joint. The measured displacement, v_m, can now be expressed in terms of $d\gamma$ as:

$$v_m = L_b d\gamma \cos\beta d\theta \tag{4.14}$$

Equations (4.12) through (4.13) are combined to express a relation between the measured displacement, v_m, and the relative rotation, $d\theta$, in terms of specimen geometry:

$$\delta\theta = \left[\frac{L_a \cos\alpha + m\cos\beta}{L_a \cos\alpha \cdot L_b \cos\beta}\right] v_m \tag{4.15}$$

The expression in brackets, a function of specimen geometry only, is called the displacement-rotation conversion factor, C_{dr}, and is computed for the specimens of the pilot study in Table 2.

4.4 Test Stability

Weld fracture must be stabilized in order to collect data measuring the moment drop per unit crack advance. The test is stable when the measured displacement for through crack propagation divided by peak load, $(dv/dP)_{meas}$, is larger than the sum of machine and specimen compliances. Otherwise, the elastic deformation of machine and specimen accelerate during crack propagation and no displacement is measured for the sudden load drop.

The required displacement from crack initiation to through crack propagation is estimated from experimentation or by Equation (4.15). Measured displacement is calculated for a web rotation assumed adequate for through crack propagation. In the

pilot experiment, for example, web rotation of 0.75° corresponding to 0.25mm displacement was assumed adequate for crack propagation. This result is divided by the peak predicted load from Chapter 3 to construct $(dv/dP)_{meas}$. Specimen compliance is discussed in the next section. Machine compliance is often provided in literature with the testing machine but may be measured as described in Appendix 2.

4.5 Specimen Compliance

The sum of specimen and machine compliance is minimized in the design phase to ensure stable fracture of the welded specimen. Specimen compliance is computed by determining the vertical displacement due to the elastic deformation of the specimen legs subjected to the reaction forces calculated in section 4.1.

For Leg A of the Lazy-L specimen, the component of the reaction force, R_a, perpendicular to the leg is $R_a \cos\alpha$. If the specimen joint is assumed fixed, then this force results in elastic deformation of the specimen leg. The magnitude of the displacement is (Crandall, 1992):

$$\delta = \frac{R_a L_a^3 \cos\alpha}{3EI} \tag{4.16}$$

where E is the Young's Modulus of the web metal and I is the moment of inertia which for the rectangular specimen leg cross section is expressed as:

$$I = \frac{w t_w^3}{12} \tag{4.17}$$

The vertical displacement at the end of the specimen leg due to the elastic deformation, δ, is $\delta\cos\alpha$. Combining this result with Equations (4.16) and (4.17), the vertical displacement of the specimen leg to elastic deformation of the leg, δ_{vert}, is:

$$\delta_{vert} = \frac{4R_a L_a^3 \cos^2\alpha}{Ewt_w^3} \tag{4.18}$$

An equivalent expression may be developed for Leg B of the specimen by substituting the reaction force, R_b, free leg length, m, and included angle, β, for the corresponding variables for Leg A in Equation (4.18). With these relations, the resulting measured displacement, v_m, due to elastic deformation of the specimen legs is computed. For a symmetric specimen in which $L_a = L_b - 2t_w$, the vertical displacements, δ_{vert}, are equal, and $v_m = \delta_{vert}$. For asymmetrical specimens, the measured displacement, vm, is the sum of the smaller vertical displacement at the leg end, δ_{vert}, and an additional vertical displacement computed in the same way as the vertical displacement due to the height rise, h_a, of Equation (4.13). For this calculation, the equivalent height rise is expressed as $\left|(\delta_{vert})_a - (\delta_{vert})_b\right|$. For simplicity, however, a conservative estimate of specimen compliance is achieved by equating v_m with the larger of the two vertical displacements at the leg ends.

4.6 Specimen Leg Limit Moment

All relations have been computed on the assumption that the specimen legs resist plastic deformation prior to weld deformation and fracture. This assumption not only guarantees weld failure, but validates the right-angle trigonometry used in the analysis. For the predicted limit moment of the chosen weld, the predicted limit load is computed

using the load-moment conversion factor, C_{lm}, developed in Section 4.2. For the corresponding reaction forces found as in Section 4.1, the predicted reaction force component perpendicular to Leg A is $R_a \cos\alpha$, while that for Leg B is $R_b \cos\beta$. When these force components are multiplied by their respective moment arms, free leg lengths L_a and m, the result is the maximum predicted moment acting on the specimen leg, M_l, which occurs close to the weld. The leg yields when the maximum stress resulting from this moment exceeds the yield stress of the web material, σ_Y.

In the elastic region, the stress distribution in a slender member subjected to bending is (Crandall, 1992):

$$\sigma_x = \frac{M_b y}{I} \tag{4.19}$$

where M_b is the bending moment, y is the distance from the neutral surface, and I is the moment of inertia. The maximum bending moment occurs at the greatest distance from the neutral surface, or for the specimen leg, where $y = t_w/2$. Combining this result with Equations (4.17) and (4.20), the criteria for no leg yielding is:

$$\begin{aligned} \sigma_Y &> \frac{6R_a L_a \cos\alpha}{w t_w^2} \\ \sigma_Y &> \frac{6R_b m \cos\beta}{w t_w^2} \end{aligned} \tag{4.20}$$

Specimen leg lengths and weld parameters are chosen to satisfy these criteria for the yield stress of the chosen web metal.

4.7 Magnitude of Weld End Effects

An important modeling assumption is the plane strain approximation; however, the weld ends of the Lazy-L specimen experience free surface effects which include out of plane deformation. Plane strain is satisfied when the weld is constrained by enough adjacent weld metal to prevent out of plane deformation. The required weld length to ensure the validity of the plane strain approximation may be determined by analyzing the scale of the free surface effect.

The scale of the free surface effect may be estimated by analyzing the effect of constraint on the yield strength of two-dimensional weld sections taken at the center and edge of the weld. As shown in Fig. 14, for stress applied in the x-direction, σ_x, the constraint of adjacent weld metal on the center section results in a stress in the y-direction, σ_y. In contrast, no stress develops in the y-direction of the end section since it is free to deform. If the effect of constraint on the resulting yield stress is small, then the free surface effect is small and the plane strain approximation is satisfied.

The yield stress of each section is expressed as a function of the root mean square of the differences among the principle stresses by the von Mises yield criterion (eg. Crandall, et al., 1992):

$$\sigma_Y = \{\frac{1}{2}[(\sigma_x - \sigma_y)^2 + (\sigma_y - \sigma_z)^2 + (\sigma_z - \sigma_x)^2]\}^{\frac{1}{2}} \tag{4.21}$$

According to Equation (4.23), the end section of the weld, subject only to σ_x, yields at $\sigma_Y = \sigma_x$. In order to satisfy the condition that the center section experiences no strain in the y-direction, $\varepsilon_y = 0$, and $\sigma_y = 0.5\sigma_x$. For this condition, Equation (4.21) provides the result that $\sigma_Y = 0.867\sigma_x$ for the center section, which suggests that the free surface effect is much less than 15% for weld material a few leg lengths from the end.

5 Specimen and Fixture Design and Fabrication

5.1 Introduction

Three configurations are available in the Lazy-L test. The first is a single fillet in predominant bending, the second is a single fillet in predominant transverse shear, and the third is the double fillet in predominant bending. Despite the differences in the predicted least upper bounds to the limit moment described in Chapter 3, the specimen design relations for the three cases are similar. Further, each configuration is tested using the same test fixtures. Therefore, a single procedure is presented for specimen and fixture design, respectively, with special note at any step for which there is difference due to the configuration.

5.2 Specimen Design

The Lazy-L specimen must meet several key requirements to provide the necessary data for accurately computing the limit moment, rotational displacement to initiation, and crack growth ductility factor. First, the specimen must be sized properly to produce a large enough moment to reach the limit moment of the weld within the available load capacity of the testing machine. Second, the specimen legs must be designed to resist yielding below the limit moment of the weld. Finally, in order to ensure a stable fracture for which unloading data may be gathered, the overall compliance must be limited to the largest slope of the load-displacement curve. The effect of design choices on these specimen characteristics are discussed below.

The design steps assume that the designer has chosen the combination of web metal and weld metal of interest. The initial choice of base metal thickness, t_W, is

suggested by the application, but may need to be increased later in the design process to stabilize the test or prevent specimen leg yielding.

Step 1: Choose weld length, w. Initial choice of weld length is driven by the plane strain requirement discussed in Section 4.6. The weld length must be several times the weld leg length to ensure plane strain and minimize the influence of weld end effects on the results. The recommended weld length is ten times the weld leg length.

As illustrated in Chapter 3, the total moment of the weld varies proportionately with weld length. Longer weld length requires either a higher machine capacity or longer, more compliant specimen legs to achieve the required moment. If the tests are to be conducted on a large capacity testing machine, then choose the recommended weld length. For smaller machines, some iteration will be necessary to determine the maximum allowable weld length. For the chosen weld length, the total required moment, M_{tot}, is:

$$M_{tot} = M_{norm}(\frac{M}{M_{norm}})w \tag{5.1}$$

where M/M_{norm} is the normalized bending moment calculated as in Chapter 3, M_{norm} is the normalizing moment for the particular Lazy-L configuration chosen, and w is the weld length.

Step 2: Choose specimen leg lengths, L. The leg lengths are chosen to achieve the required moment, M_{tot}, at a load within the capacity of the testing machine. For the selected leg lengths, compute the reaction forces as a function of the applied load, P, using Equations (4.1)-(4.6). With these reaction forces, express the moment per unit weld length, M_W, as a function of applied load, P, using the appropriate relation from Section 4.2. From this expression, determine if the total moment, $M_{tot} = M_W \cdot w$, may be

achieved within the machine load capacity. In order to minimize specimen compliance and prevent the onset of leg yielding, select the minimum leg lengths which provide the required moment.

Step 3. Calculate specimen compliance, $(dv/dP)_S$. Specimen compliance is computed using Equations (4.16)-(4.18). Specimen compliance must be minimized since the test will be unstable if the sum of specimen and machine compliances is greater than the anticipated load drop per unit displacement of the weld. Machine compliance is computed as described in Appendix 3 and weld compliance is estimated from prior experiments or as the measured displacement for through crack propagation at the peak test load. From Equation (4.18), specimen compliance is a strong function of specimen leg length and a strong inverse function of web metal thickness. If the minimum leg lengths have been chosen for the required M_{tot} in step 2, then the specimen compliance may be reduced by increasing the web metal thickness, t_w. If web metal thickness may not be increased, then the weld length must be decreased in order to reduce M_{tot} and allow for shorter specimen leg lengths.

Step 4. Check specimen leg yielding. Equation (4.20) provides the criteria for no yielding in the specimen legs. Stress in the specimen legs is a strong inverse function of web metal thickness, but a weaker function of specimen leg length. If web metal thickness can not be increased to satisfy the leg yielding criteria, then leg length must be reduced. If the leg length is already minimized from step 2, then the weld length must be decreased to reduced M_{tot} and allow for shorter specimen leg lengths.

5.3 Specimen Fabrication

Fabrication techniques are selected which best represent the application for which the Lazy-L test is being conducted. The two specimen legs are machined square at the dimensions, L, w, and t_w chosen above. The welding procedure, process parameters and degree of surface preparation are chosen to match the application. Several important considerations during welding include weld fit-up, deformation and edge cooling effects.

The theory developed in Chapter 3 does not account for changes in the slip lines and corresponding bounds to the weld limit moment due to variations in root gap. Although root gap of up to two millimeters is allowed in shipbuilding applications for which the leg length is nine millimeters (Middaugh, 1994), the theory assumes a close-fit weld for which the root gap is negligible.

The development also assumes that the specimen legs are welded at right angles; however, deformation due to welding causes the specimen legs to fold over toward the side of the joint which is welded. Deformation is minimized by securely tack welding the legs in place at right angles before welding the specimen. Tack welds are placed on the side of the joint opposite the weld and may also be placed at the ends as shown in Fig. 15. Once the weld is made, the specimen is machined to remove the tack weld material. The most desirable alternative is to machine the specimen legs two inches wider than the design width, w, to allow extra surface for tack welds on the side of the joint opposite the weld. After welding, the entire specimen is machined to width w to remove the extra material. (Masubuchi, 1994) This method also removes the start and stop of the weld which cool at a slightly different rate than the remainder of the weld and are usually not of consistent quality. Fig. 16 illustrates a representative machine drawing of the as-fabricated Lazy-L specimen.

5.4 Fixture Design

A principal advantage of the Lazy-L test is that all configurations use the same simple test fixtures. As shown in Fig. 1, these are a base plate, load applying plate, and three 3/4-round supports. Fixtures are designed to reduce friction and resist yielding at the highest anticipated test loads.

The 3/4-round supports reduce friction and indentation while ensuring that the reaction force vector remains orthogonal to the base plate for any degree of specimen leg rotation. They are designed to the length of the longest anticipated weld length, w, and sized to resist yielding at peak loading. For cylinder length large compared to diameter, the maximum compressive stress at the point of contact between the 3/4-round and the plate is (Roark, 1989):

$$\sigma_{max} = 0.591\sqrt{\frac{pE}{D}} \tag{5.2}$$

given in terms of the load per unit length p, Young's modulus E, diameter D, and a constant for dimensions in pounds and inches. Since equation (5.2) assumes similar Young's modulus and Poisson's ratio for the plate and 3/4-round, a hardened steel with high yield strength, σ_Y, is chosen for all fixtures. For this material, compute the diameter, D, which satisfies the criterion: $\sigma_Y > \sigma_{max}$. If the required diameter is prohibitively large, then select are new material for which the criterion is satisfied at a reasonable diameter. For example, the 3/4-rounds described in Chapter 6 for the pilot experiment were fabricated using one inch diameter T1 steel. Note that fixture compliance is assumed negligible compared to machine and specimen compliance. Any available plate thickness in the range of 1/4 to one inch is recommended.

5.4 Fixture Fabrication

In order to provide stability and accommodate large specimen deformation, the base plate is fabricated to a width greater than the longest anticipated weld length, w, and a length roughly twice the specimen leg length. Since anticipated horizontal displacement of the top 3/4-round is small, the load applying plate may be machined as a square the same width as the base plate. All plates are surface ground and polished to reduce friction with boundary lubrication during the test.

The 3/4-rounds are turned to diameter D and then drilled along the axis using a 1/8-inch diameter bit. A 90° wedge of material is removed using a band saw and milling machine to complete the fabrication. The drilling procedure creates a rounded notch which relieves the stress concentration in the event of uneven loading caused by a specimen leg that is not properly squared. Fig. 17 illustrates a representative machine drawing for the 3/4-round supports.

6 Data Analysis and Interpretation

The parameters of interest in the Lazy-L test are the limit moment, slip line displacement to crack initiation and the crack growth ductility factor, Dg, defined as the inverse of crack growth per unit slip line displacement. This section demonstrates how these are computed from measured Lazy-L load-displacement data and expressed in terms of universal weld parameters including weld geometry and mean normal stress across the slip line. In this form, the Lazy-L test results may be applied to other fillet weld failure modes including pure tension and peeling for which experiments are less practical.

6.1 Moment-Rotation from Load-Displacement

The data conversion factors developed in Chapter 4 are used to convert measured load-displacement data to moment (per unit weld length)-rotation data. Measured loads are multiplied by the load-moment factor for the specimen, C_{lm}, and divided by the weld length, w. Corresponding displacements are multiplied by the displacement-rotation factor, C_{dr}. (See Table 2)

6.2 Slip Line Displacement

The rotational displacement above is the rotation of one Lazy-L specimen leg with respect to the other. For small angles, the displacement along the arc of sliding is the product of the rotational displacement and the radius of the arc:

$$u_s = r\delta\theta \tag{6.1}$$

Slip line displacements for the pilot study are reported in Table 3.

6.3 Crack Growth Ductility Factor

The crack growth ductility factor, $D_g = du_s / da$, is a measure of the slip line displacement per unit crack advance needed for calculating the tear resistance of welds in tension according to(McDonald, 1994):

$$R_{weld} = D_g k_f d^2 \tag{6.2}$$

where R_{weld} is the tear resistance, or tearing work per unit weld length. For a slip line displacement from Equation (6.1), the ductility factor is constructed by computing the crack advance (or reduction of ligament) for the corresponding drop in moment. In the case of single fillet bending, for example, the moment drop is related to the change in ligament by the normalized limit moment Equation (3.4). Crack growth ductility is reported for the stable tests of the pilot study in Table 4.

6.4 Lazy-L Parameters in Terms of Mean Normal Stresses

Lazy-L test results expressed in term of the mean normal stress across the crack tip are independent of the test configuration and applicable to other loadings. McClintock (1994) has developed equations for the mean normal stress at the fillet root as functions of the slip arc angles (eg. Table 1) and the fillet shear strengths for each of the three Lazy-L configurations. With angles in radians, the mean normal stress at the root of the single fillet in bending Fig. 6 is:

$$\frac{\sigma_C}{2k_f} = (\frac{\phi_D}{\pi/2} - 1) + (\phi_C - \phi_D) \tag{6.3}$$

Similarly, the mean normal stress for the single fillet in transverse shear Fig. 7 is:

$$\frac{\sigma_A}{2k_f} = (\frac{\phi'_B}{\pi/2} - 1) + (\phi_A - \phi_B) \tag{6.4}$$

where $\phi'_B = \phi_B + \pi/4$ in order to measure from the fillet surface rather than the horizontal as in Equation (3.7). Finally, the two mean normal stresses for the double fillet in bending Fig. 8 are:

$$\frac{\sigma_C}{2k_f} = (\frac{\phi_D}{\pi/2} + \frac{1}{2}) + (\phi_C - \phi_D) \qquad \frac{\sigma_A}{2k_f} = (\frac{\phi_B}{\pi/2} - \frac{1}{2}) + (\phi_A - \phi_B) \tag{6.5}$$

Graphs of displacement to initiation or crack growth ductility against corresponding normal stresses depict the relationships for use in general fillet weld design.

7 Lazy-L Experiment and Results

7.1 Test Specimens

An experimental study was conducted to validate the Lazy-L design as a feasible alternative to more costly and difficult methods such as finite element analysis for determining limit moment, displacement to initiation, and crack growth ductility. The combination of 20mm LR-EH36 plate and E7016 stick electrode were selected since prior research by Tanker Safety Project members (ie. Kirkov, 1994) had shown it to be of interest to the shipping community. Further, consistent material selection allows comparison of results from a number of different experiments.

Twelve specimens were fabricated to include at least two of each configuration, one with 9mm weld leg length and the other with 6mm leg length. Specimen leg length, L, and weld length, w, were varied in an effort to stabilize the tests and demonstrate the robustness of the results to changes in specimen geometry. Table 1 lists the measured dimensions, reaction forces, and data conversion factors for each of the specimens tested.

7.2 Experimental Procedure

The specimens were ruptured in compression on a 20,000 lb. capacity Instron 1125 testing machine equipped with Labtech Notebook data acquisition software. Details of calibration and data acquisition procedures are provided as Appendix 5. Support fixtures included three one inch diameter 3/4-round supports machined from T1 steel, and hardened steel flat-plate grips provided as fixtures with the Instron 1125. Points of contact between the 3/4-rounds and plates were well lubricated with a combination of heavy oil and pulverized Teflon in a solvent. During testing, the influence of friction was tested by reversing the direction of the crosshead to create a hysteresis in the output. For

a narrow hysteresis, the effect of friction is shown to negligible. Tests were run until zero load or until the incremental load drop became very small. Ruptured specimens were surface polished and tested for hardness both within the weld and base metal.

A peculiarity of the testing machine used is that the crosshead displacement is computed by Notebook as the product of the crosshead speed and the elapsed test time. As illustrated by the triangular shapes of load-displacement curves of Appendix 2, the result is that both tensile and compressive crosshead displacements appear positive in the output. To create the hysteresis loop, the data sets were processed on Microsoft Excel spreadsheets to convert positive crosshead displacement increments during unloading to negative displacements increments in the output.

7.3 Experimental Measurements

A plot of limit moment/unit weld length versus rotational displacement is presented in Appendix 4 for each of the specimens tested. Limit moments are calculated from the raw load-displacement data by multiplying the measured load by the load-moment conversion factor, C_{lm}, and dividing by the weld length, w. Corresponding rotational displacement data are found by multiplying the measured displacements and the displacement-rotation conversion factor, C_{dr}, for each test. (See Table 2) Notice that for each configuration, the assumption of negligible friction is confirmed by a narrow hysteresis loop.

The six single fillet bending tests are characterized by a steep load rise in the elastic region before plastic deformation and load drop due to fracture. The shape of the curve for the first 6mm fillet in bending appears inconsistent in that there is negligible plastic deformation before fracture. Although this might normally indicate fracture below the yield point of the weld, the load data for this test are also inconsistently high. Load data for the single fillets in transverse shear are more uniform; however, the displacement to

crack initiation varied significantly. Also, notice from the steep load drops that the crack growth was not stabilized. Spikes in the data for the single 6mm fillet in transverse shear result from the rupture of Teflon shims that were used in an effort to further reduce the effect of friction. The 6mm double fillet tests are characterized by rupture of the fillet in shear followed by reloading and subsequent fracture of the remaining fillet in bending. Notice that the 9mm double fillet specimen did not rupture at the weld due to excessive specimen leg yielding.

7.4 Experimental Outputs

As described in Chapter 6, the Lazy-L experiment produces the limit moment, slip line displacement to initiation, and crack growth ductility factor. Experimental normalized limit moments are listed in Table 3. They are constructed by dividing the peak moment for each specimen by the appropriate normalizing moment expressed as a function of weld leg length and fillet or web shear strength. Slip line displacement to initiation, also listed in Table 3, is computed according to Equation (6.1).

Crack growth ductility may be computed only for those specimens for which crack propagation was stabilized. In the pilot experiment, this includes all six of the single fillet bending specimens. Observation of the fracture surfaces in these specimens reveal that the crack advances nearly along the weld throat. As shown in Figure (20), this may result from the interaction of two symmetrical arcs of sliding which are alternately active. The resulting fracture is similar to that of an unequally grooved plate of weld metal in bending with a half back-angle of 90°. Neglecting changes in half back-angle, the least upper bound arc solution (McClintock, Kim, Parks, 1995) relates the moment to the ligament by:

$$M = 1.380(k_f b^2 / 2) \tag{7.1}$$

where b is the ligament. The change in ligament is computed by Equation (7.1) for arbitrarily selected changes in moment. The rotational displacement corresponding to this change in moment is used to compute the slip line displacement from Equation (6.1). Table 4 illustrates the computation of crack growth ductility for five of the single fillet bending cases where the reference moments are chosen as the moment at crack initiation, M_{init}, and 90% of the moment at crack initiation. Lower values challenge the small angle approximation for Equation (7.1). Predicted values for crack growth ductility are 0.24 for evenly matched welds and 0.12 for overmatched welds. (Lyman, 1969)

8 Conclusions and Recommendations for Future Work

8.1 Conclusions

1. Limit moment, displacement to initiation, and crack growth ductility are critical fillet weld parameters in predicting the integrity of fillet welded joints subject to web folding, pure tension and peeling.

2. The Lazy-L Test is a practical, simple, and inexpensive means of measuring limit moment, displacement to initiation, and crack growth ductility. Fully plastic fracture mechanics allows extrapolation of test results to other loading conditions.

3. Experimental results indicate that the least upper bound to the limit moment from a single arc approximation of the plastic flow field in the fillet under predicts the limit moment by 10-20% for the single fillet in transverse shear and the double fillet in bending. The limit moment for single fillet bending is significantly over predicted for 9mm welds, and 10-20% over predicted for 6mm welds.

4. Experimental crack growth ductility estimates from stabilized single fillet bending specimens modeled as unequally grooved plates of fillet metal in bending with 90° half back-angle are within +/-20% of the predicted value of 0.12 for overmatched welds.

5. The Lazy-L Test should be further developed for consideration as a standard test of limit moment, displacement to initiation and crack growth ductility for use in the design and qualification of fillet welds for service.

8.2 Recommendations for Future Work

1. Further experimentation with the Lazy-L configuration is recommended to develop an extensive experimental database for a range of materials and geometries. Stabilized tests of single fillet transverse shear are needed to estimate crack growth ductility from this configuration. Tests of the effect of penetration and weld metal matching on strength and ductility parameters are recommended.

2. Develop an experimental method of measuring crack direction during the test or from analysis of fractured specimens. Model the crack growth vector as a function of mean normal stress across the crack tip for incremental changes in slip line displacement. For a crack assumed to propagate along the slip line, consider changes in the slip line computed to yield the least upper bound to the limit moment for each increment of crack advance.

3. Consider new models of the slip line field for single fillet bending including a pair of symmetrical arcs ending in a constant state region at the free surface. Determine limit moment correlation for new model.

4. Relax small angle assumption by developing specimen geometry as a function of the measured displacement.

5. Correlate limit moment, displacement to initiation, and ductility factor from Lazy-L tests with applicable results of finite element analysis, transversely welded beam test, and tension tests.

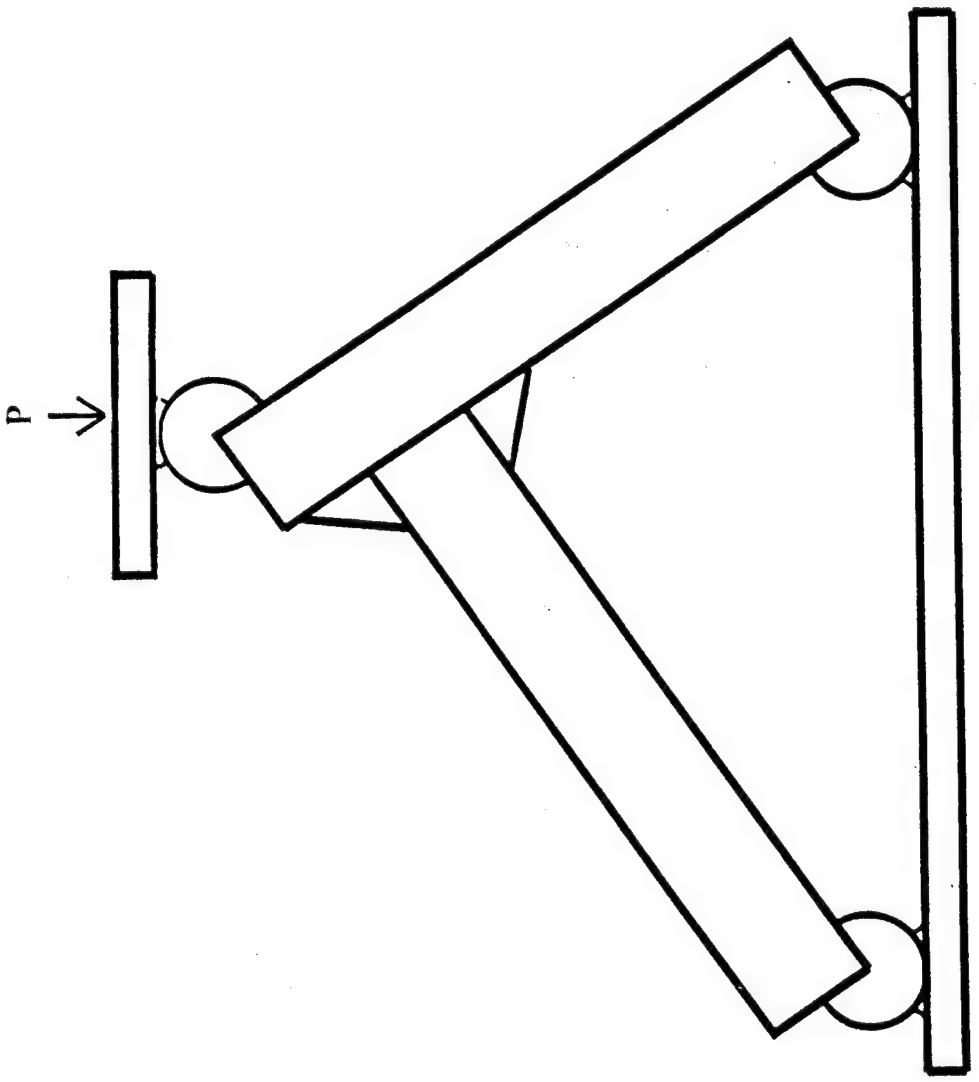

Figure 1: Lazy-L Test Configuration

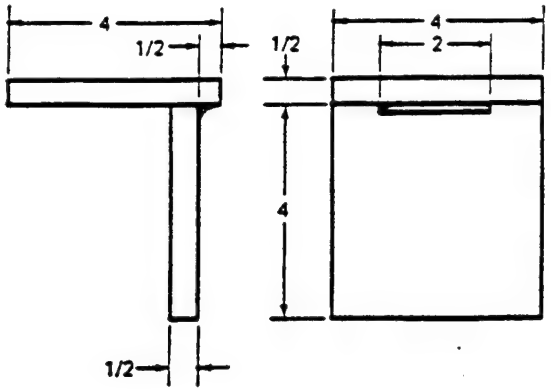

Fig. 5.47–Fillet-weld-break specimen–tacker qualification

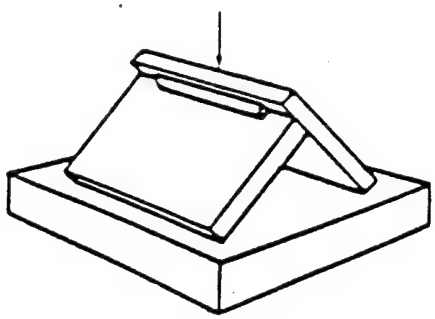

Fig. 5.48–Method of rupturing specimen–tacker qualification

FIGURE 30C.8
Test No. 3—Fillet-weld Test

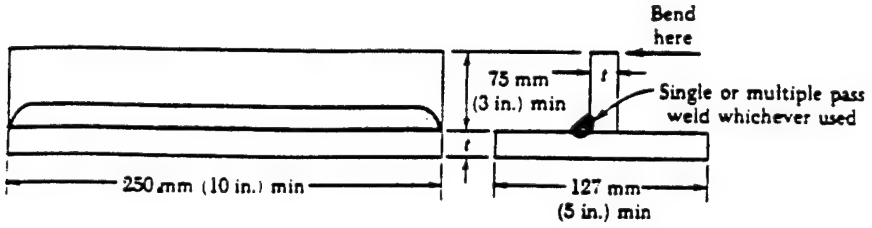

Notes

1 For procedure qualifications, t = 9.5 mm (⅜ in.) for construction materials up to 19.1 mm (¾ in.). For construction material over 19.1 mm (¾ in.) t = thickness of material
2 Base and standing web is to be straight and in intimate contact and securely tacked at ends before fillet-weld is made, to insure maximum restraint.
3 The test plate may be flame cut into short sections to facilitate breaking open.

Requirements

The fillet is to be of the required contour and size, free from undercutting and overlapping. When broken as indicated, the fractured surface is to be free from cracks. Visible porosity, incomplete fusion at the root corners and inclusions may be acceptable, provided the total length of these discontinuities is not more than 10% of the total length of the weld.

Figure 2: American Bureau of Shipping Fillet Weld Break Tests

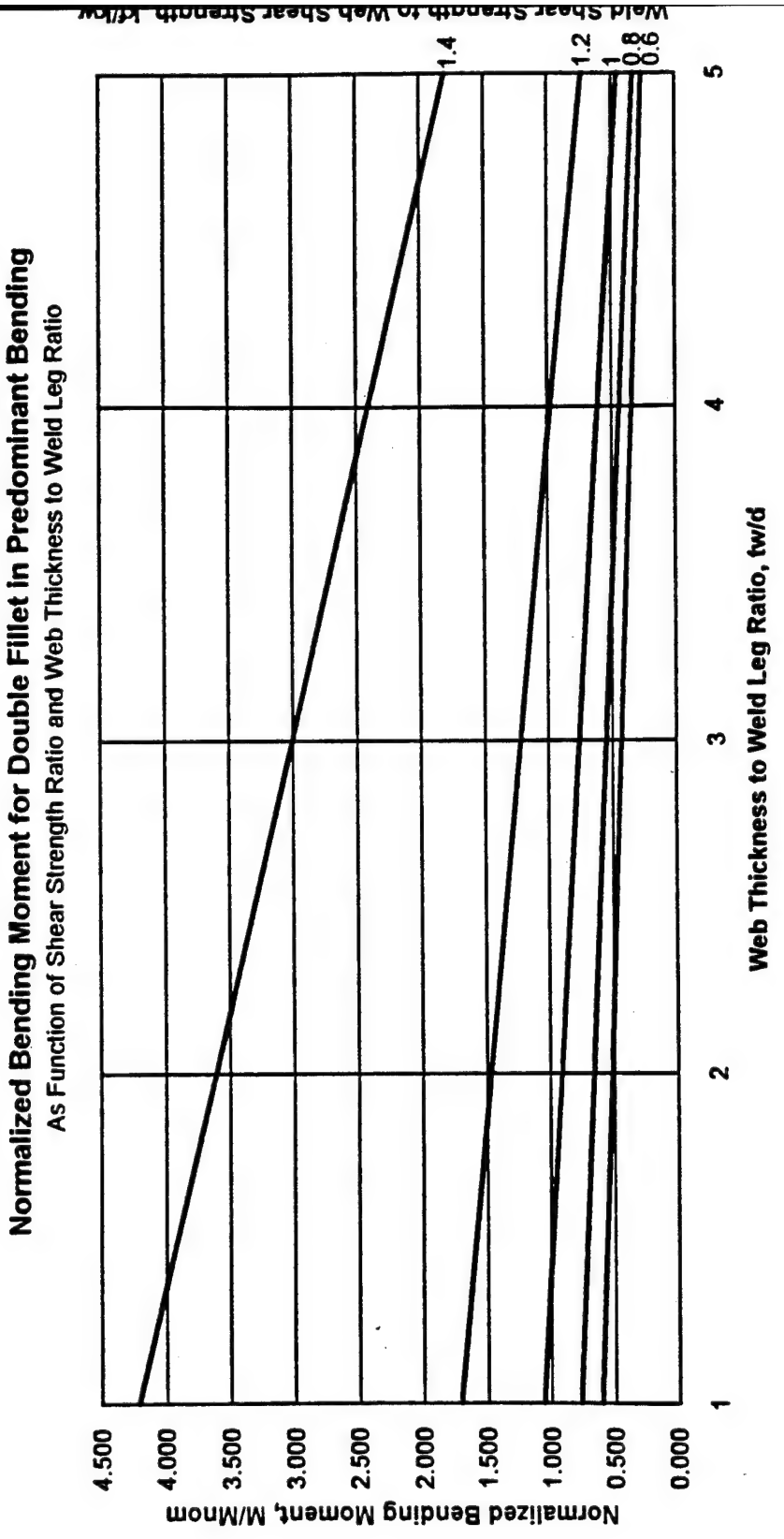

Figure 3: Normalized Bending Moments for Double Fillet in Predominant Bending

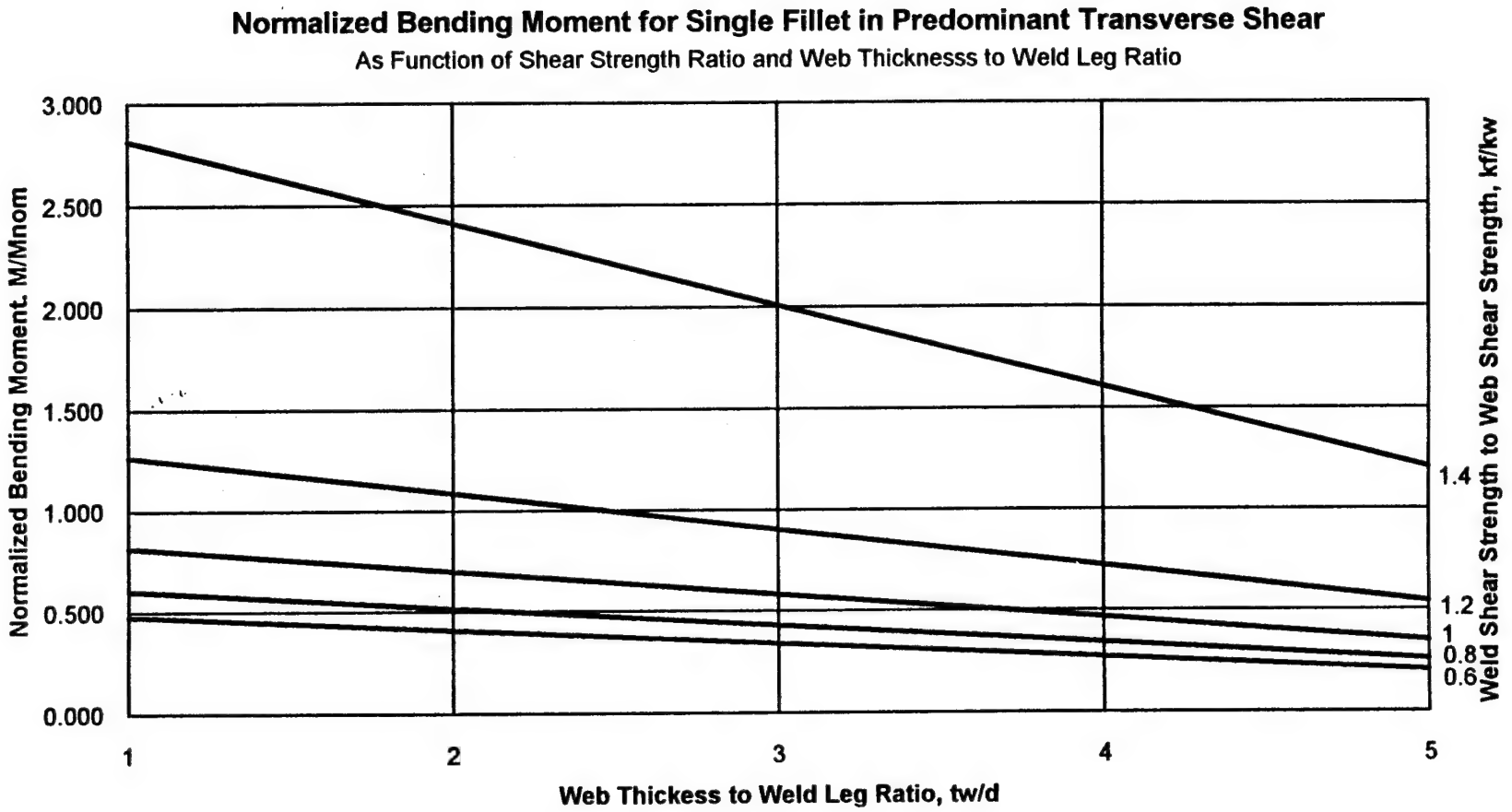

Figure 4: Normalized Bending Moments for Single Fillet in Predominant Transverse Shear

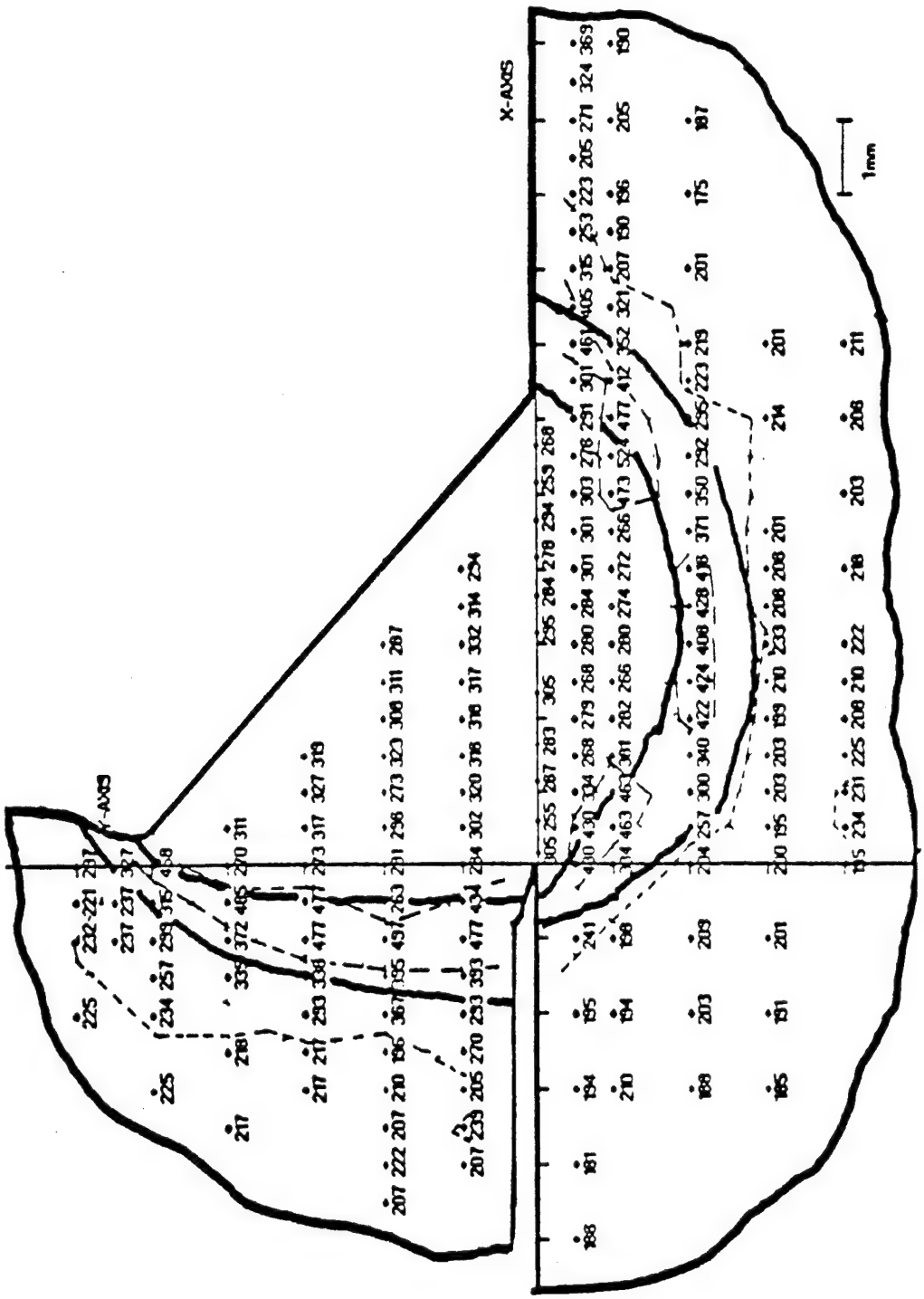

Figure 5: Hardness Distribution in a Fillet Weld (Middaugh, 1994)

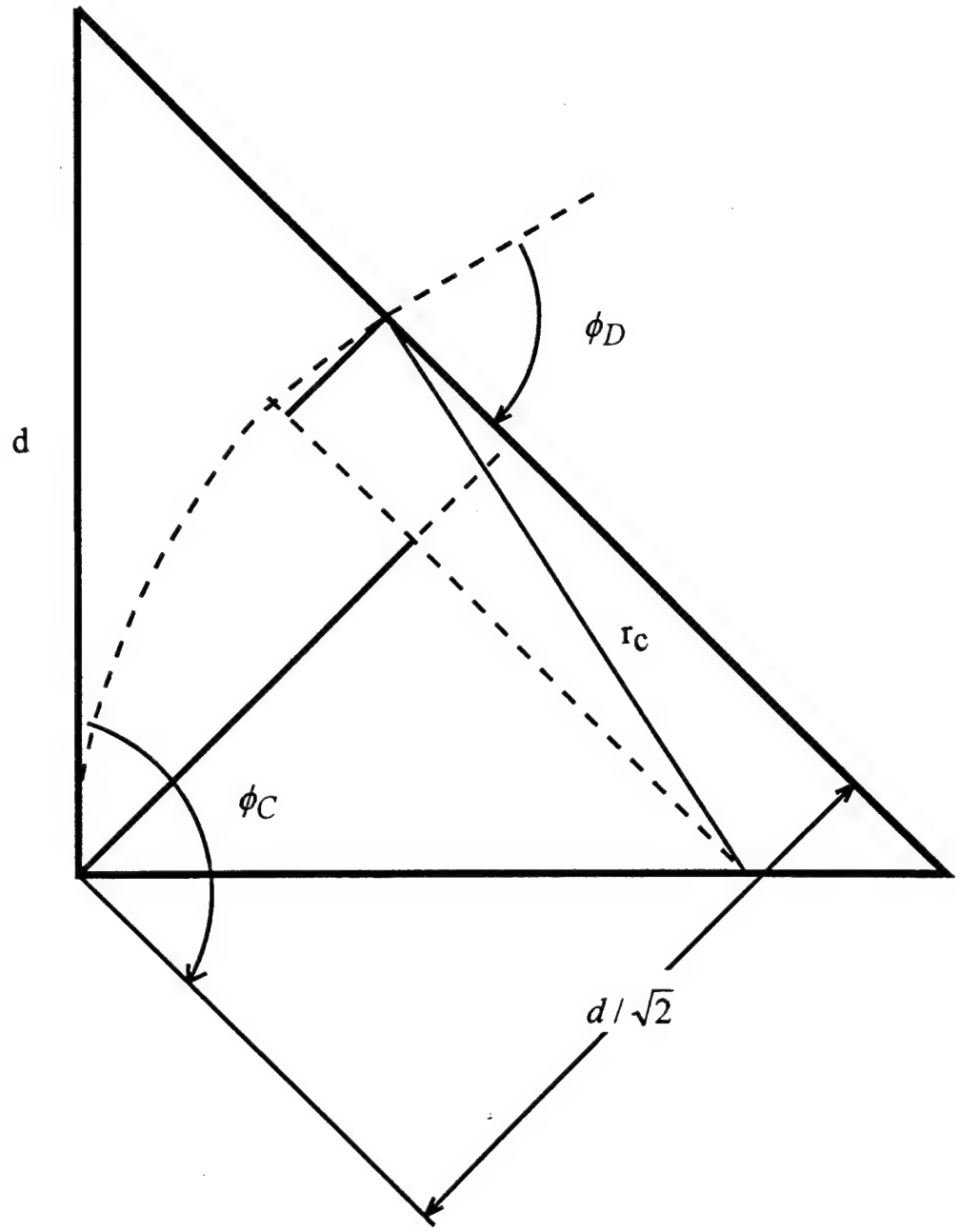

Figure 6: Geometry of Single Fillet in Predominant Bending

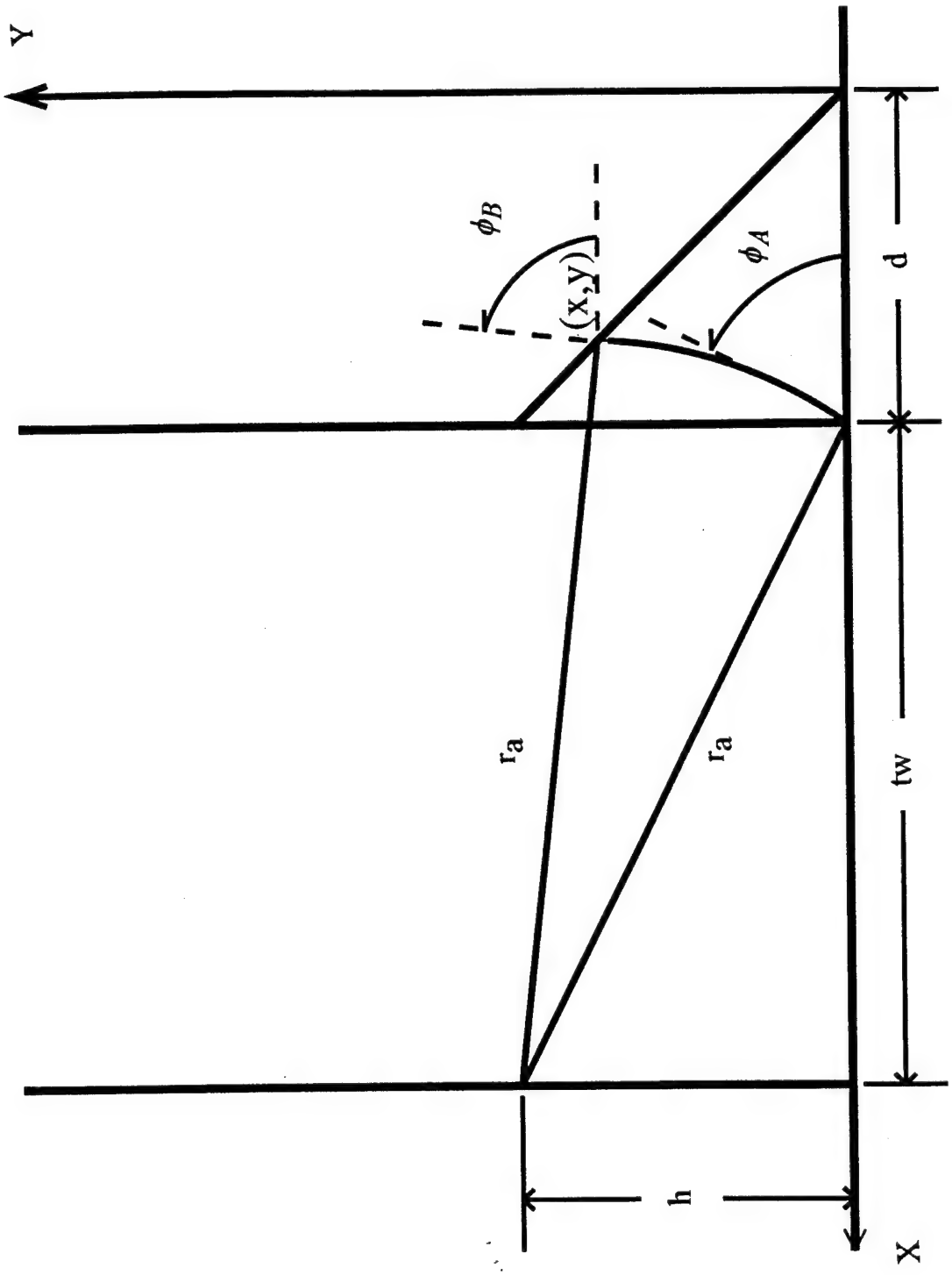

Figure 7: Geometry of Single Fillet in Predominant Transverse Shear

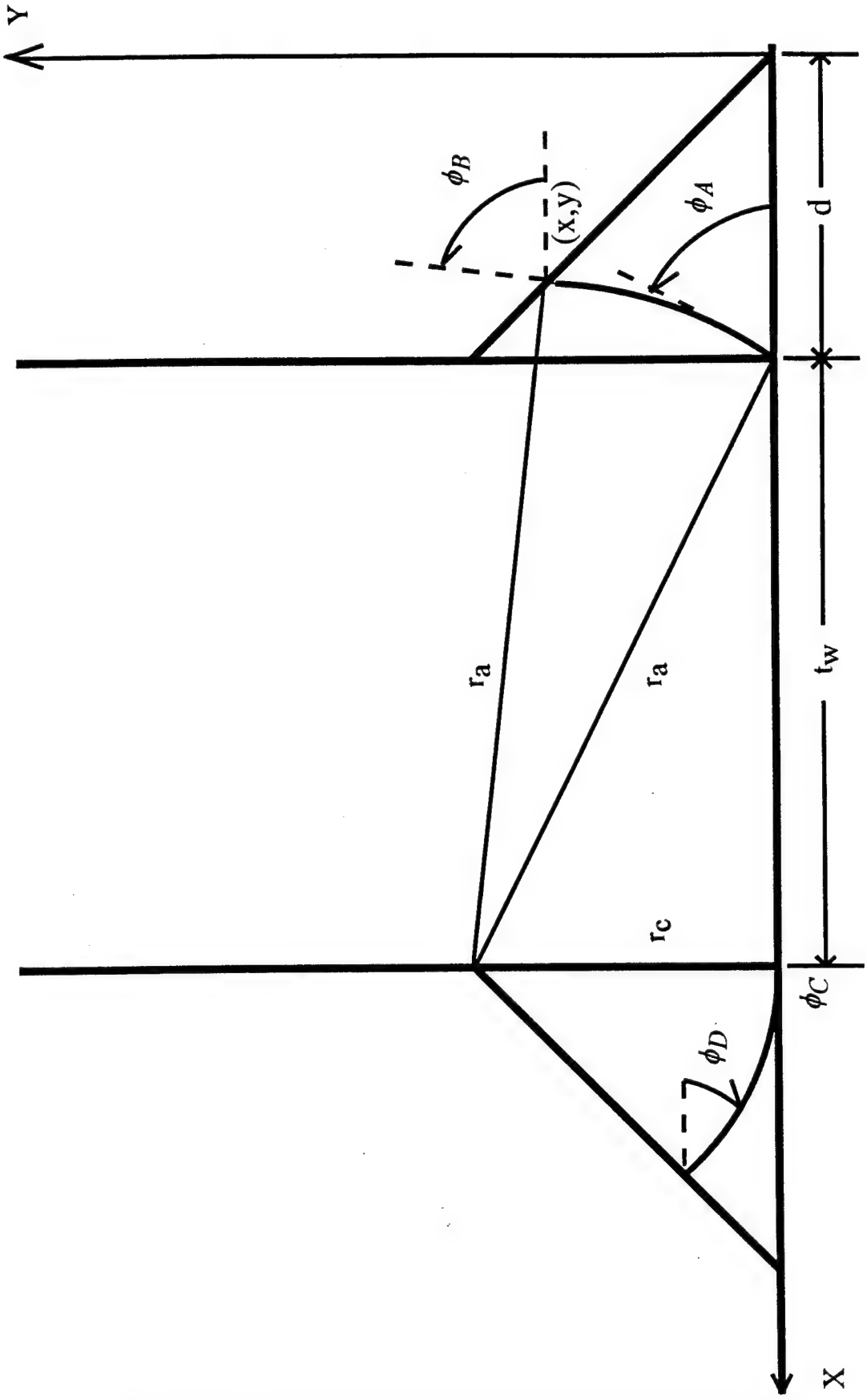

Figure 8: Geometry of Double Fillet in Predominant Bending

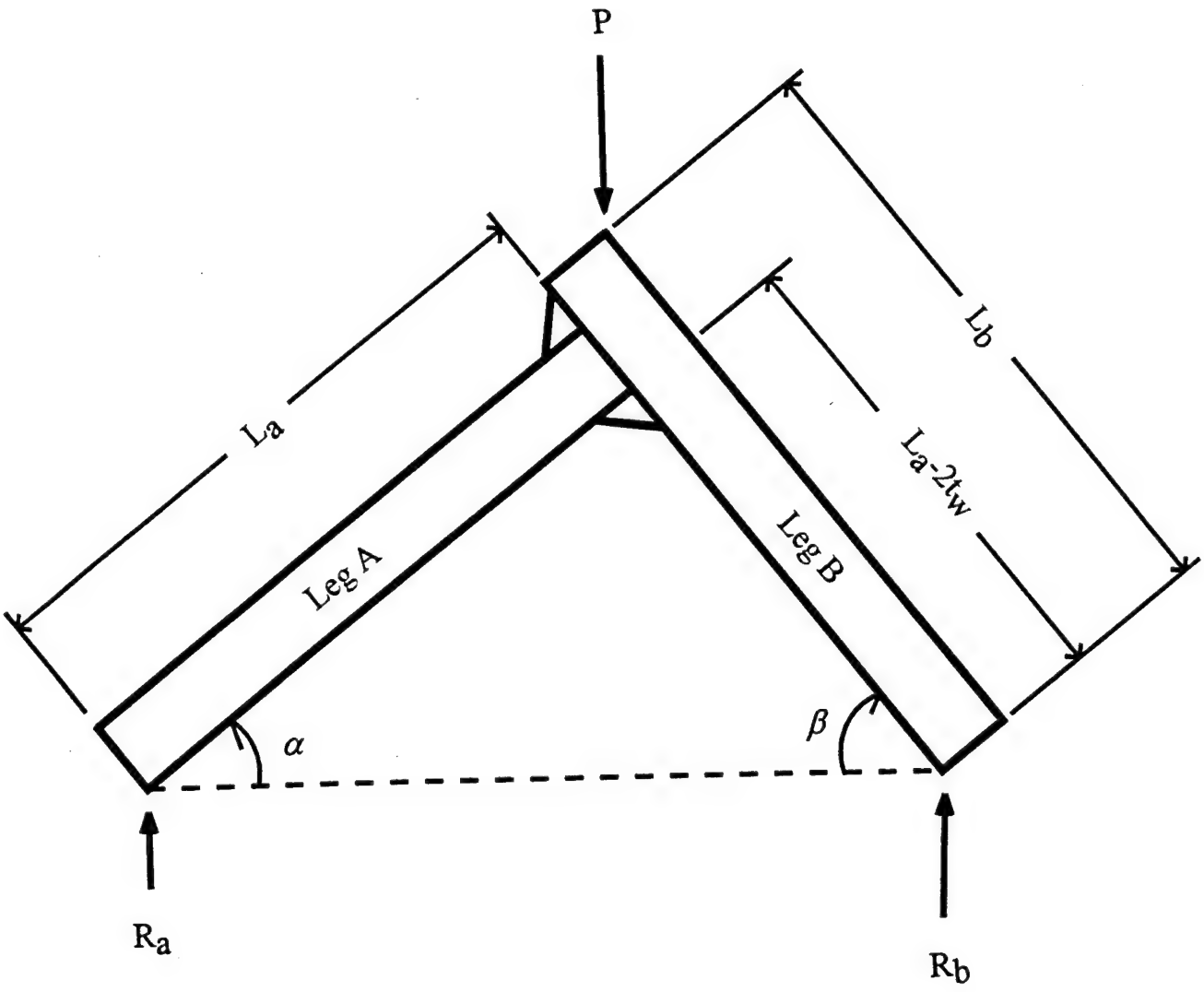

Figure 9: Overall Lazy-L Specimen Geometry

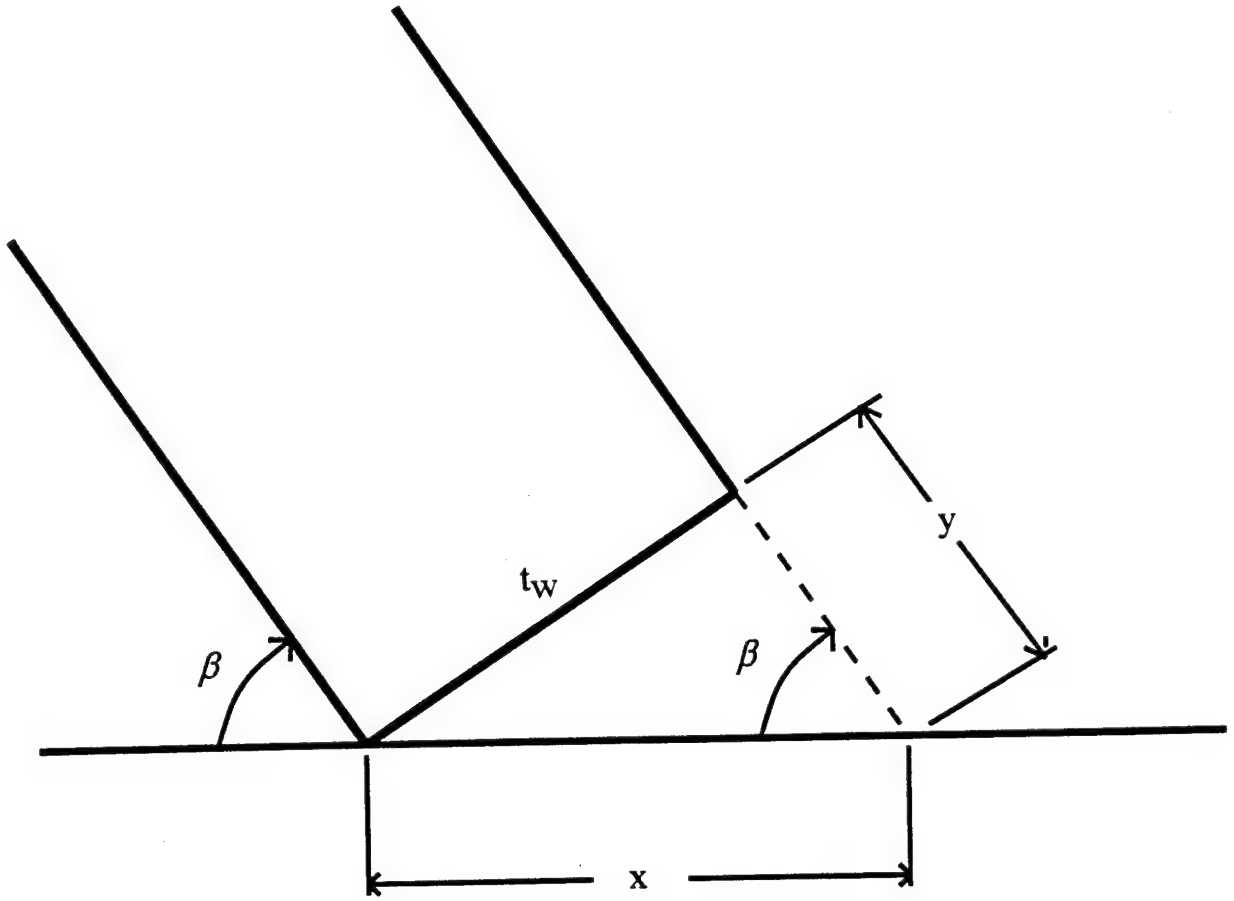

Figure 10: Geometry for Calculating Moment Arm of Reaction Force

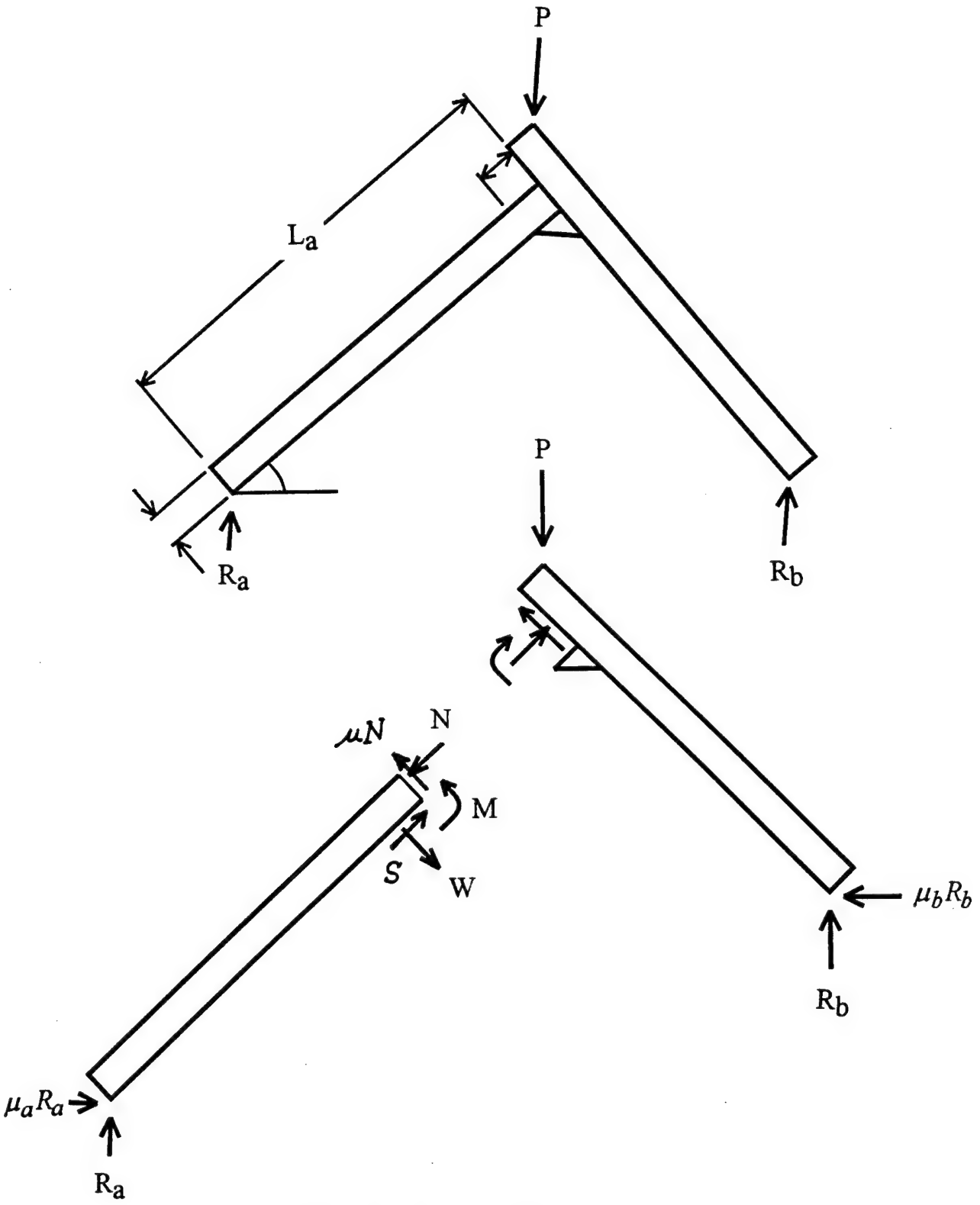

Figure 11: Diagrams for Evaluating Moment
of Single Fillet in Predominant Transverse Shear

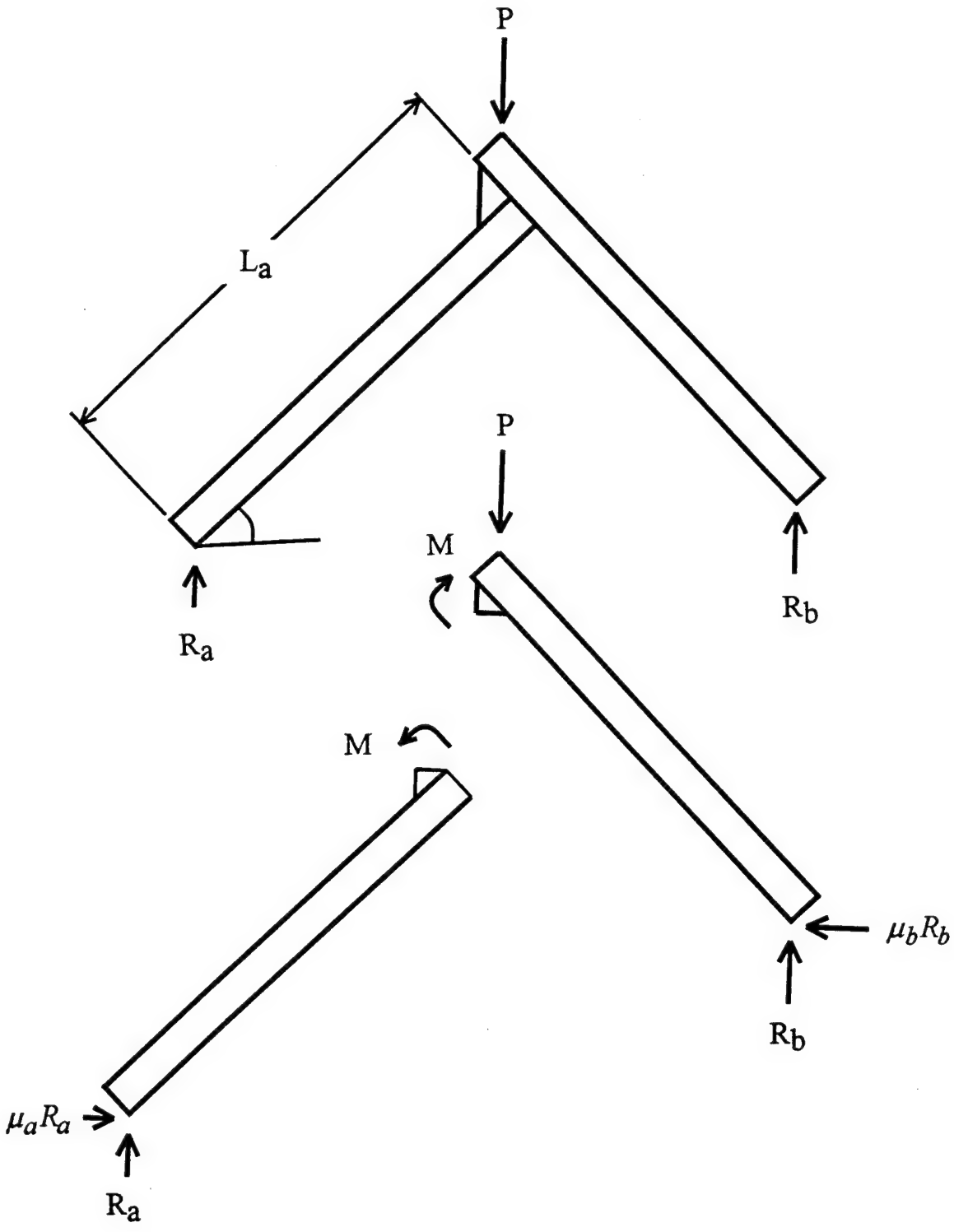

Figure 12: Diagrams for Evaluating Moment
of Single Fillet in Predominant Bending

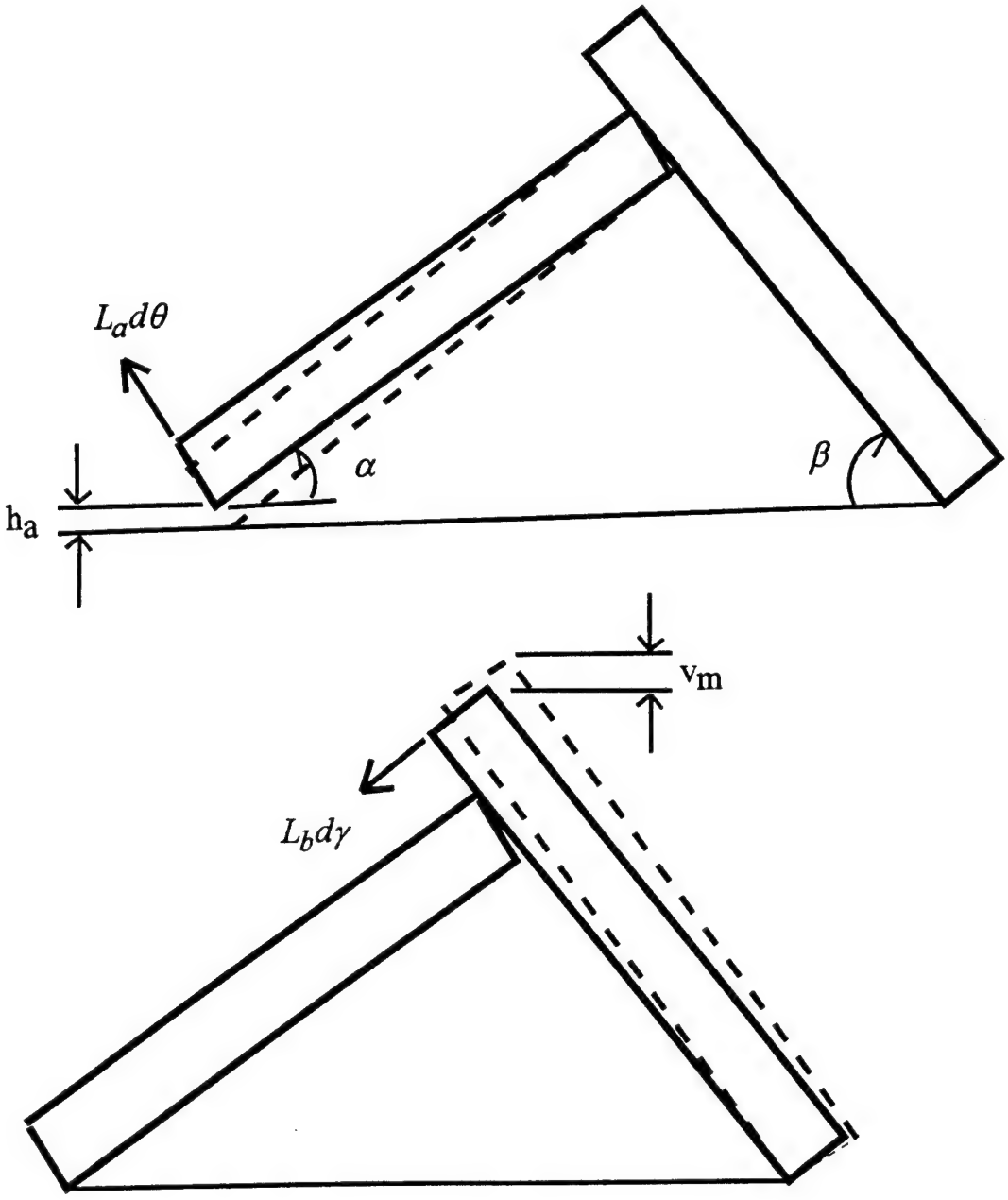

Figure 13: Geometry for Evaluating Weld Rotation from Measured Displacement

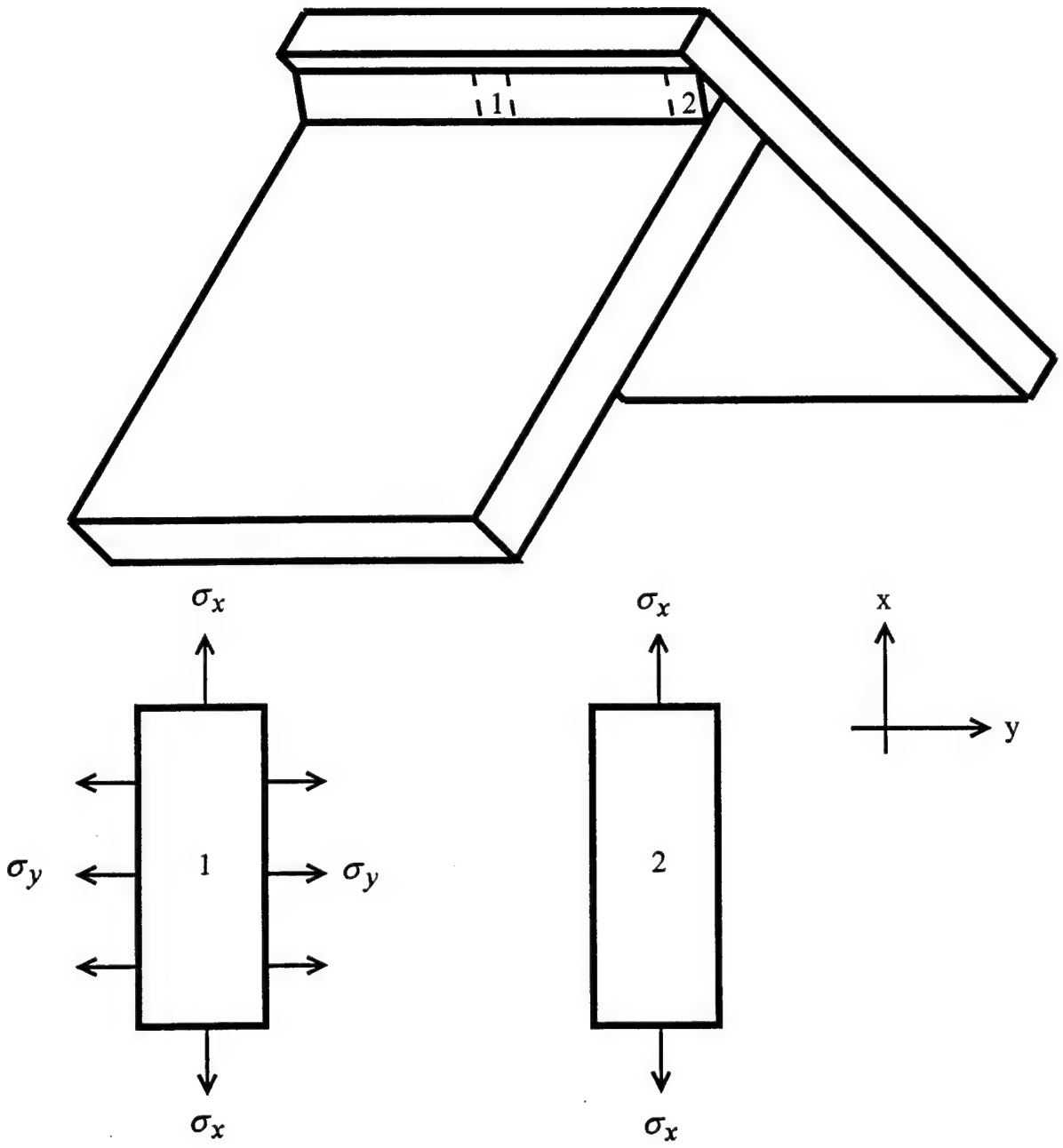

Figure 14: Model for Free Surface Effect at Weld End

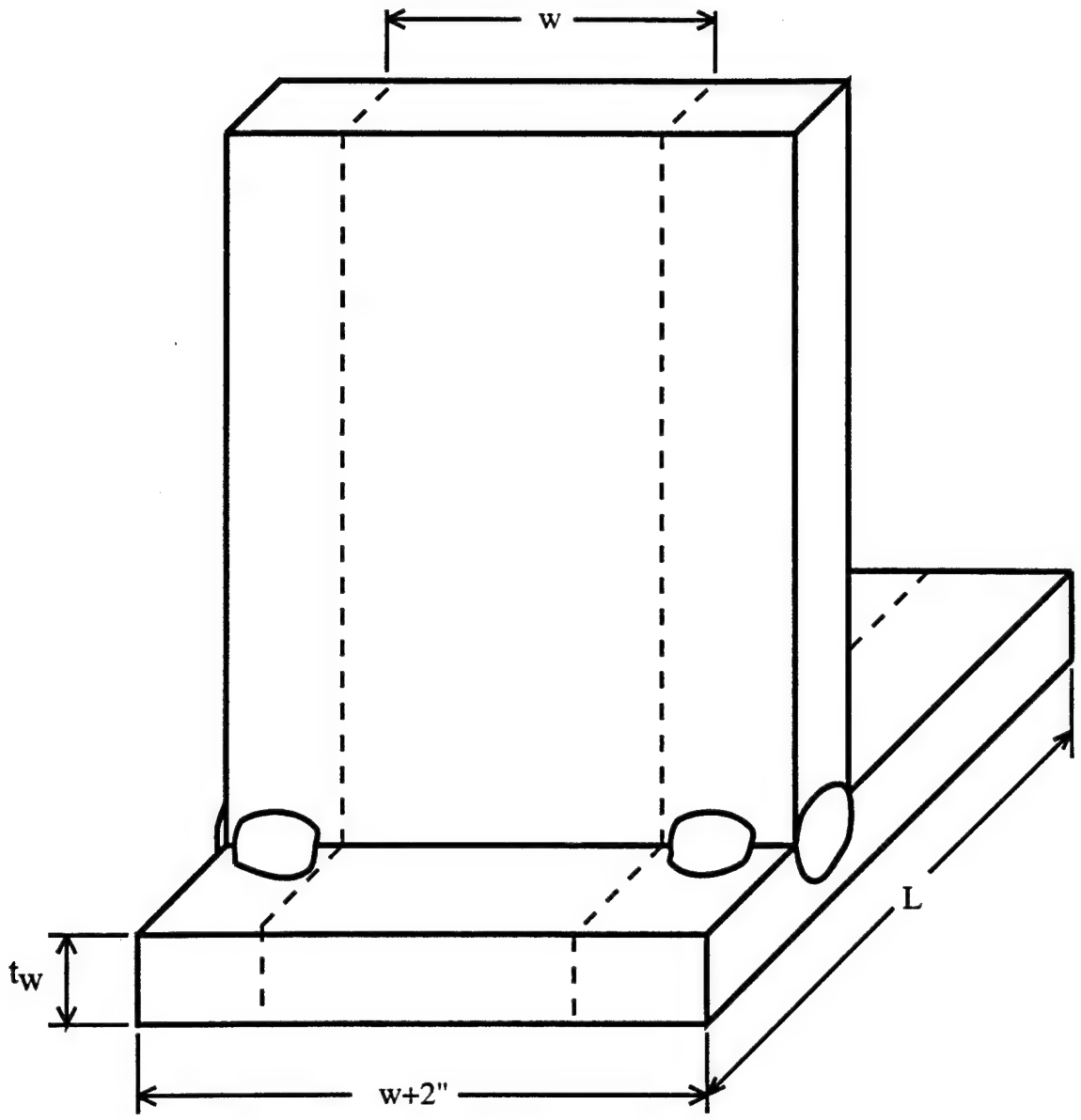

Figure 15: Suggested Tack Welds for Fabrication

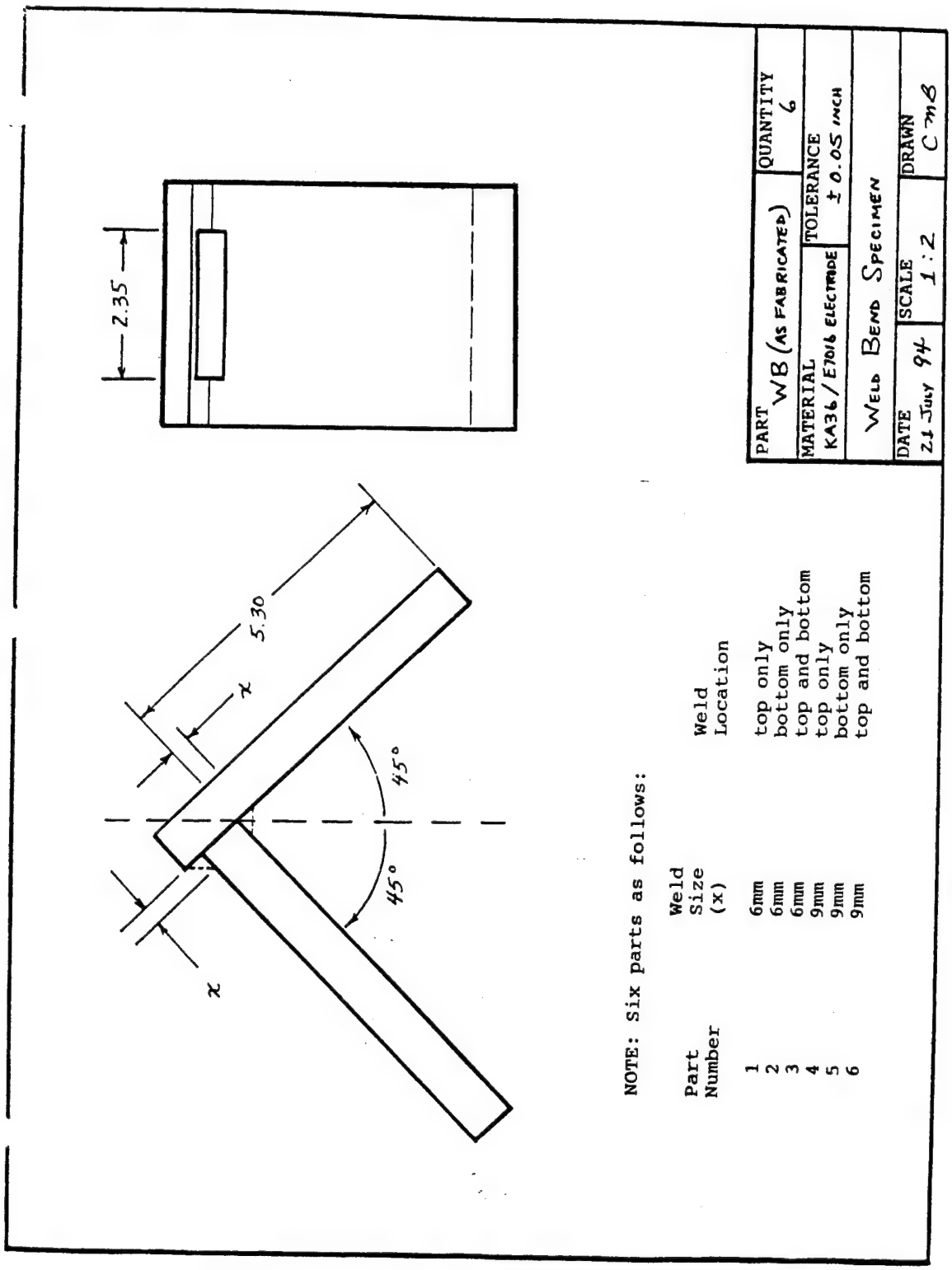

Figure 16: Representative Machine Drawing of Lazy-L Specimen

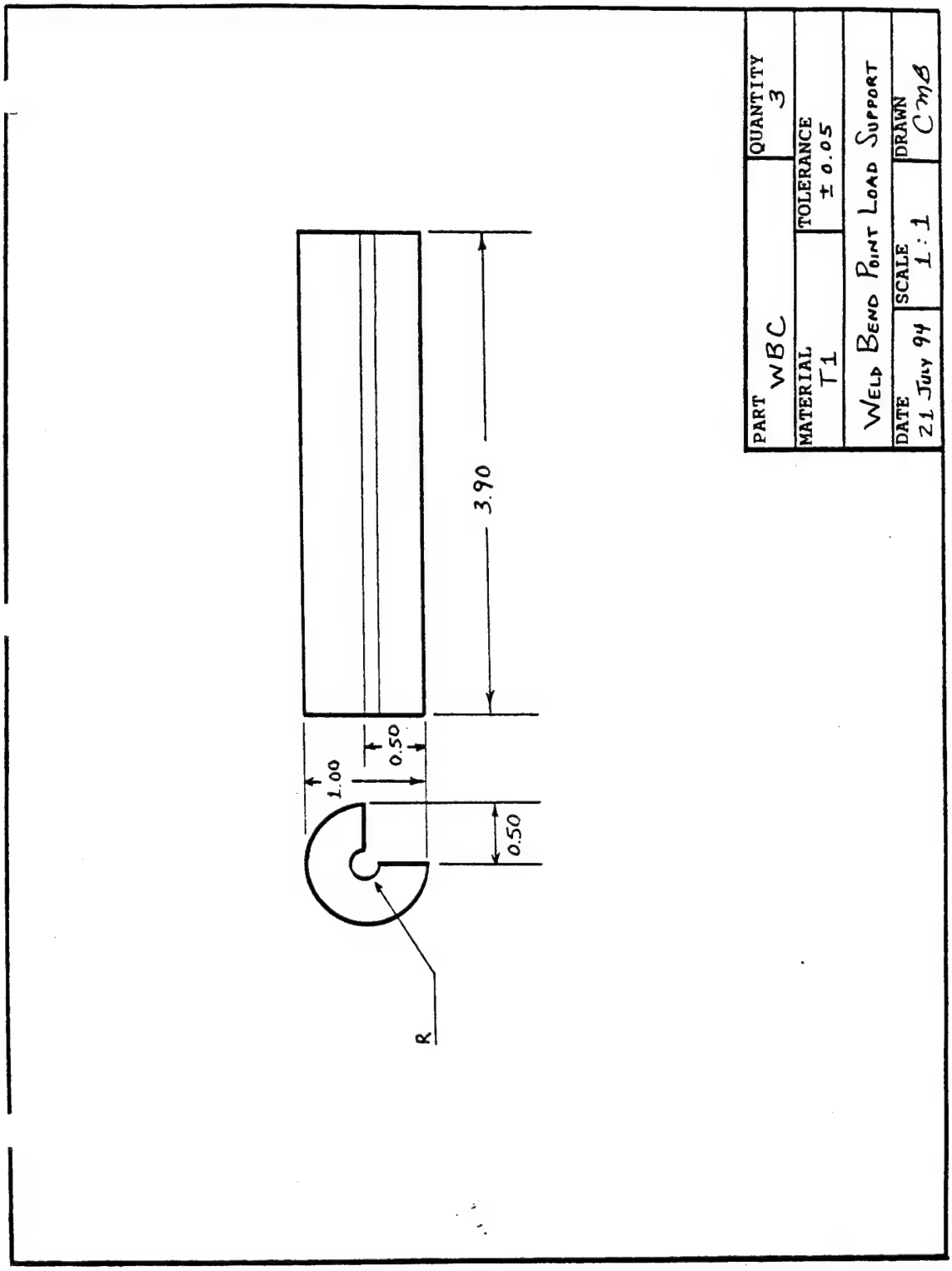

Figure 17: Representative Machine Drawing of 3/4-Round Support

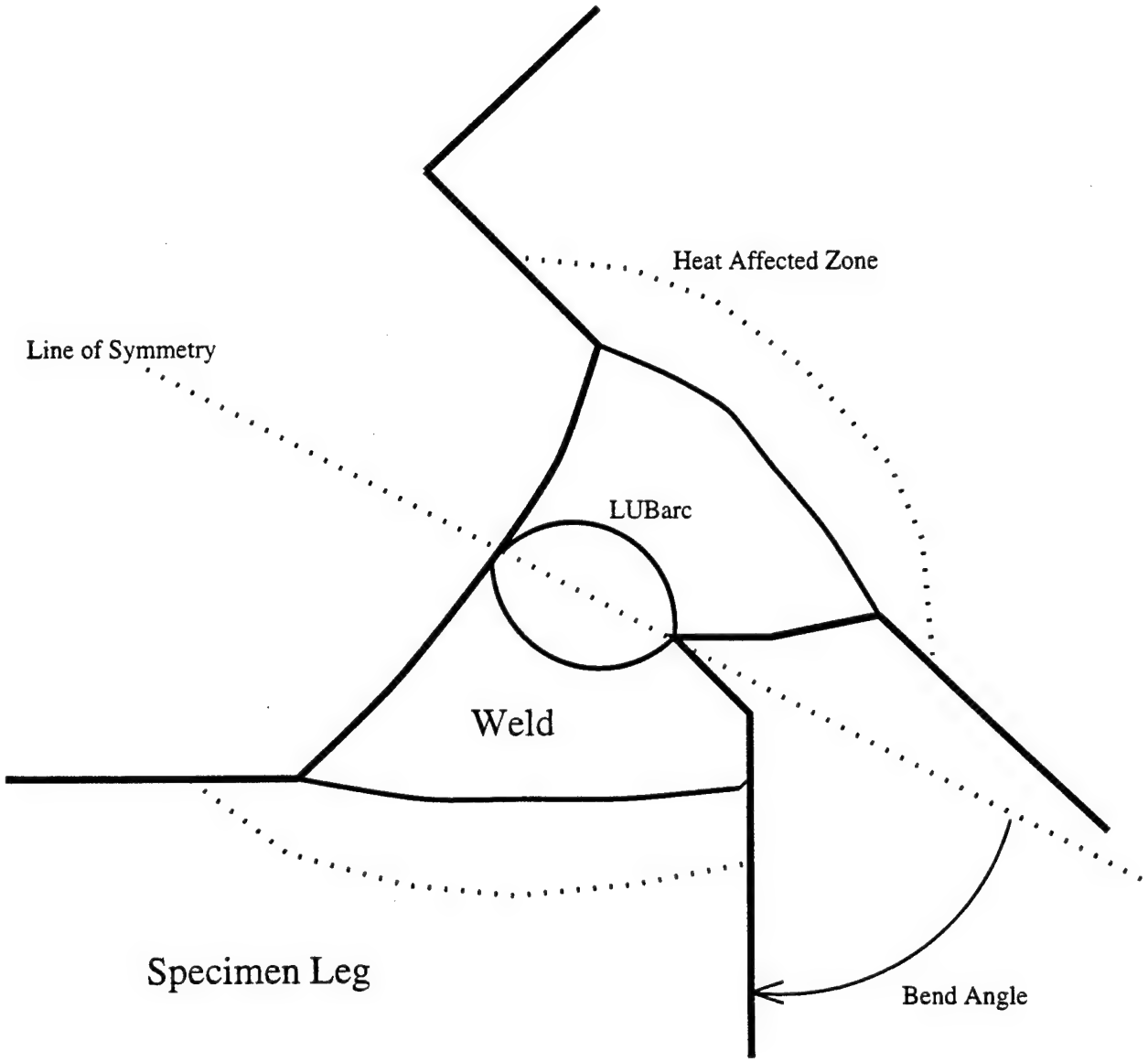

Figure 18: Observed Crack Direction in Single Fillet Bending

Table 1: Slip Line Parameters and Predicted Normalized Bending Moments

For web thickness of 20mm; fillet and web shear strengths from Appendix 3

Specimen <by weld leg>	Radius, rc <mm>	Radius, ra <mm>	Phi A <rad>	Phi B <rad>	Phi D <rad>	M/Mnorm
Single Fillet Bending ($M_{NORM} = k_f d^2/4$)						
6mm (all)	2.62	N/A	N/A	N/A	0.422	1.475
9mm (all)	3.95	N/A	N/A	N/A	0.422	1.475
Single Fillet Trans. Shear ($M_{NORM} = k_w t_w^2/2$)						
6mm (1st)	10.04	22.38	1.106	1.314	N/A	1.002
9mm (1st)	11.04	22.85	1.066	1.375	N/A	1.646
9mm (2nd)	11.04	22.85	1.066	1.375	N/A	1.485
Double Fillet Bending ($M_{NORM} = k_w t_w^2/2$)						
6mm (1st)	4.08	20.41	1.370	1.648	1.130	1.405
6mm (2nd)	4.08	20.41	1.370	1.648	1.130	1.277
9mm (1st)	5.72	20.80	1.292	1.698	1.203	1.956

Table 2: Specimen Dimensions. Reaction Forces, and Data Conversion Factors

Specimen <by weld leg>	Specimen Legs La <mm>	Lb <mm>	Angles Alpha (Eqn. 4.1) <rad>	Beta (Eqn. 4.2) <rad>	Reaction Forces Ra/P (Eqn. 4.6)	Rb/P (Eqn. 4.6)	Arc Radius Rc (Eqn. 3.9) <mm>	Load-Moment Conversion Factor Clm (Eqn. 4.10) <mm>	Disp.-Rot. Conversion Factor Cdr (Eqn. 4.17) <mm>
Single Fillet Bending									
6mm (1st)	89.9	89.1	0.582	0.989	0.300	0.700	2.64	18.55	0.0293
6mm (2nd)	165.0	165.0	0.686	0.885	0.417	0.583	2.64	47.17	0.0160
6mm (3rd)	160.0	160.0	0.682	0.888	0.414	0.586	2.64	45.35	0.0165
9mm (1st)	165.0	166.0	0.689	0.881	0.422	0.578	3.95	47.03	0.0159
9mm (2nd)	166.0	167.0	0.690	0.881	0.422	0.578	3.95	47.39	0.0158
9mm (3rd)	160.0	160.0	0.682	0.888	0.414	0.586	3.95	44.93	0.0165
Single Fillet Trans. Shear									
6mm (1st)	164.0	164.0	0.685	0.886	0.417	0.583	10.10	44.40	0.0161
9mm (1st)	112.0	117.0	0.660	0.910	0.395	0.605	11.05	26.63	0.0223
9mm (2nd)	164.0	166.0	0.692	0.878	0.425	0.575	11.05	44.62	0.0159
Double Fillet Bending									
6mm (1st)	163.0	164.0	0.688	0.883	0.420	0.580	4.08	46.26	0.0161
6mm (2nd)	164.0	164.0	0.685	0.886	0.417	0.583	4.08	46.35	0.0161
9mm (1st)	165.0	165.0	0.686	0.885	0.417	0.583	5.72	46.18	0.0160

References

American Bureau of Shipping (ABS), 1991, Rules for Bulding and Classing Steel Vessels, Chapter 30.

Chakrabarty, J. Theory of Plasticity. 1987, McGraw-Hill, New York.

Crandall, S.H., Dahl, N.C., and Lardner, T.J., An Introduction to the Mechanics of Solids, 1992, McGraw-Hill Inc.

"Federal Register", Dec. 1990, Vol. 55, No. 234, U.S. Federal Printing Office.

Kim, Y.J., McClintock, F.A., and Parks, D.M., "Global Equilibrium of the Least Upper Bound Circular Arcs Applied to Fracture Mechanics", February, 1993, *J. Mech. Phys. Solids*.

Kirkov, K.D., "Tearing Resistance for Fillet Welds in Ships Exposed to Grounding - A Full Scale Test and Cost Implications", May, 1994, S.M. Thesis, M.I.T. Department of Ocean Engineering.

Krumpen R.P. Jr., and Jordan, C.R., "Updating of fillet weld strength parameters for Commercial Shipbuilding", 1984, *Ship Structural Committee Report 323*.

Lyman, 1969, Metals Handbook.

Masubuchi, K. M.I.T. Professor of Ocean Engineering, 1994, personal communication.

McClintock, F.A. "Fully Plastic Fracture Mechanics for Fillet Welded T- Joints", 1994, Joint M.I.T.-Industry Consortium on Tanker Safety, Report No. 26.

McClintock, F.A., Kim, Y.J., and Parks, D.M., "Tests and Analyses for Fully Plastic Fracture Mechanics of Plane Strain Mode I Crack Growth", 1995, *Fracture Mechanics, 26th Vol., ASTM STP 1256*.

McClintock, F.A., Kim, Y.J, and Parks, D.M, "Criteria for Plane Strain, Fully Plastic Quasi-Steady Crack Growth", 1995, *Int. J. Fracture.*

McDonald, H.A. "Required Strength and Tear Resistance for Fillet Welds in Ships Exposed to Grounding or Collision Loads", 1993, S.M. Thesis, M.I.T. Department of Ocean Engineering.

Middaugh, R.A., 1993, personal communication.

Yang, W.C., ed., Roark's Formulas for Stress and Strain. 6th ed. McGraw-Hill, New York, 1989.

Wierzbicki, T., Peer, D.B., and Rady, E., "The Anatomy of a Tanker Grounding", *Marine Technology*, 1993, Vol. 30, No. 2, pp.71-78.

Appendix 1: Minimization of Normalized Limit Moments

A1.1 Computer Methods

For fillet shear strength, web metal shear strength, and web metal thickness, the normalized bending moments presented as Equations (3.5), (3.12), and (3.15) are minimized in terms of the normalized radius of curvature, R_c/d. For simplicity, minima are calculated by entering the equations of Chapter 3 in a spreadsheet and evaluating over a range of R_c/d and t_w/d as needed. Tables (A1.1)-(A1.3) illustrate the use of Microsoft Excel spreadhseets for each of the three Lazy-L configurations, Figs. 6-8. Note that the height, h, of the arc focus in the single fillet in shear is the equivalent of R_c for the remaining cases.

A1.2 Spreadsheet Codes

The following codes for computed values are presented for the benefit of the reader who wishes to write spreadsheets to solve for the limit moments of the various configurations. The following codes are expressed in a format accepted by Microsoft Excel and may not be appropriate for all spreadsheet applications. For clarity, the equation number is provided from which each code is developed. Note that column and row references, although not printed in the tables, correspond alphabetically and numerically to those depicted. Also note that R_c, and its equivalent, h, are not computed values but are idependently assumed variables.

Single Fillet in Predominant Bending

d rc

Phi D Eqn. 3.3 {=ACOS(B3/(A11:A36*SQRT(2)) - (1/SQRT(2)))}

B11:B36

r_c d ϕ_c

M/M_{nom} Eqn 3.5 {=4 * ((A11:A36/B3)^2) * ((135*PI()/180) - B11:B36)}

Single Fillet in Predominant Transverse Shear

r_c t_w d

X,Y Eqn. 3.10 {=((A13:A38+(B4+B5)) - SQRT(A13:A38^2 +

B13:B38 (2*A13:A38*(B4+B5)) - (B4+B5)^2 + (2*B4^2)))/2}

t_w^2 R_c^2

R_a Eqn. 3.9 {=SQRT(B4^2+A13:A38^2)}

C13:C38

r_c r_a

Phi A Eqn. 3.7 {=ACOS(A13:A38/C13:C38)}

D13:D38

r_c x r_a

Phi B Eqn. 3.8 {=ACOS((A13:A38-B13:B38)/C13:C38)}

E13:E38

kf r_a^2 $\phi_B - \phi_A$ kw t_w^2

M/M_{nom} Eqn. 3.12 {=2*D5*((C13:C38^2)*(E13:E38-D13:D38))/(D4*(B4^2))}

Double Fillet in Predominant Bending

Codes for X/Y, Phi A, and Phi B are same as for Single Fillet Shear.

d r_c

Phi D Eqn. 3.14 {=(135*PI()/180)-ACOS((B5/(A13:A38*SQRT(2))) -(COS(

F13:F38 45*PI()/180)))}

kf r_c^2 ϕ_D r_a^2

M/M_{nom} Eqn. 3.15 {=2*D5*(((A13:A38^2)*F13:F38) + ((C13:C38^2)*

ϕ_B ϕ_A kw t_w^2

(E13:E38-D13:D38)))/(D4*(B4^2))}

Table A1.1: Minimization of Normalized Bending Moment for Single Fillet in Predominat Bending

Constants

d <mm>:	6.00
M:	kf (Phi C-Phi D) Rc^2
Mnorm:	kf *d^2/4

Calculated Variables (see Figure 6)

Arc Radius, rc <mm>	Phi D <rad>	M/Mnorm < >	
2.50	0.142	1.538	
2.52	0.217	1.509	
2.54	0.272	1.494	
2.56	0.317	1.485	
2.58	0.356	1.479	
2.60	0.391	1.476	
2.62	0.422	1.475	<
2.64	0.451	1.475	
2.66	0.478	1.477	
2.68	0.503	1.479	
2.70	0.527	1.482	
2.72	0.550	1.485	
2.74	0.571	1.489	
2.76	0.592	1.494	
2.78	0.611	1.499	
2.80	0.630	1.504	
2.82	0.648	1.509	
2.84	0.665	1.515	
2.86	0.682	1.522	
2.88	0.698	1.528	
2.90	0.714	1.535	
2.92	0.729	1.542	
2.94	0.744	1.549	

Table A1.2: Minimization of Normalized Bending Moment for Single Fillet in Predominant Transverse Shear

Constants (for 6mm specimen)

web thickness, tw<mm>:	20.0
weld leg length, d <mm>:	6.0
web metal shear strength, kw<lbs/mm^2>:	35.4
fillet metal shear strength, kf <lbs/mm^2>:	68.0
M:	kf (Phi B-Phi A) ra^2
Mnom:	2kwtw^2/4

Calculated Variables (see Figure 7)

Height, h <mm>	X, Y <mm>	Radius, ra <mm>	Phi A <rad>	Phi B <rad>	M/Mnorm < >	
10.00	4.362	22.361	1.107	1.316	1.001731	
10.02	4.359	22.370	1.106	1.315	1.001727	
10.04	4.355	22.379	1.106	1.314	1.001726	<
10.06	4.352	22.388	1.105	1.313	1.001726	
10.08	4.349	22.397	1.104	1.312	1.001728	
10.10	4.346	22.406	1.103	1.311	1.001732	
10.12	4.343	22.415	1.102	1.310	1.001738	
10.14	4.340	22.424	1.102	1.309	1.001745	
10.16	4.336	22.433	1.101	1.308	1.001754	
10.18	4.333	22.442	1.100	1.307	1.001765	
10.20	4.330	22.451	1.099	1.306	1.001778	
10.22	4.327	22.460	1.098	1.305	1.001792	
10.24	4.324	22.469	1.098	1.304	1.001808	
10.26	4.321	22.478	1.097	1.303	1.001826	
10.28	4.318	22.487	1.096	1.302	1.001846	
10.30	4.314	22.496	1.095	1.301	1.001867	
10.32	4.311	22.506	1.094	1.301	1.001890	
10.34	4.308	22.515	1.094	1.300	1.001915	
10.36	4.305	22.524	1.093	1.299	1.001941	
10.38	4.302	22.533	1.092	1.298	1.001969	

Table A1.3: Minimization of Normalized Bending Moment for Double Fillet in Predominant Bending

Constants (for 2nd 6mm specimen)

web thickness, tw<mm>:	20.0
weld leg length, d <mm>:	6.0
web metal shear strength, kw<lbs/mm^2>:	36.5
fillet metal shear strength, kf <lbs/mm^2>:	69.2
M:	kf [(Phi D) rc^2+(Phi B-Phi A) ra^2]
Mnorm:	2kwtw^2/4

Calculated Variables (see Figure 8)

Radius, rc <mm>	X, Y <mm>	Radius, ra <mm>	Phi A <rad>	Phi B <rad>	Phi D <rad>	M/Mnom < >	
4.00	5.673	20.396	1.373	1.653	1.147	1.27719	
4.02	5.667	20.400	1.372	1.652	1.141	1.27717	
4.04	5.660	20.404	1.371	1.650	1.136	1.27715	
4.06	5.654	20.408	1.371	1.649	1.130	1.27714	
4.08	5.648	20.412	1.370	1.648	1.125	1.27714	<
4.10	5.642	20.416	1.369	1.646	1.119	1.27715	
4.12	5.636	20.420	1.368	1.645	1.114	1.27716	
4.14	5.630	20.424	1.367	1.644	1.109	1.27717	
4.16	5.625	20.428	1.366	1.643	1.103	1.27720	
4.18	5.619	20.432	1.365	1.641	1.098	1.27723	
4.20	5.613	20.436	1.364	1.640	1.093	1.27727	
4.22	5.607	20.440	1.363	1.639	1.088	1.27731	
4.24	5.601	20.445	1.362	1.637	1.083	1.27736	
4.26	5.595	20.449	1.361	1.636	1.078	1.27742	
4.28	5.589	20.453	1.360	1.635	1.074	1.27748	
4.30	5.583	20.457	1.359	1.634	1.069	1.27755	
4.32	5.577	20.461	1.358	1.632	1.064	1.27763	
4.34	5.572	20.465	1.357	1.631	1.059	1.27771	
4.36	5.566	20.470	1.356	1.630	1.055	1.27780	
4.38	5.560	20.474	1.355	1.628	1.050	1.27789	

Appendix 2: Measurement of Test Machine Compliance

Before testing, machine compliance must be determined. Machine compliance, expressed as $(dv/dP)_m$, is a measure of the incremental crosshead displacement for a given load increment. This displacement, due to the elastic behavior of the crosshead and crosshead supports, is often negligible; however, in experiments such as the Lazy-L test which are characterized by large loads and small measured displacements, crosshead displacement becomes significant.

Machine compliance data is often included in literature from the manufacturer, but varies with the crosshead position and the direction and orientation of the test; therefore, it should be measured at the time of testing for a particular test configuration.

A common technique for measuring machine compliance in tension is to collect load-displacement data while the upper and lower grips are rigidly connected. The inverse slope the resulting curve is the machine compliance. The greatest risk associated with this method is that the maximum capacity of the load cell may be exceeded if there is any error in the calibration of the data acquisition system. A much safer technique exists for measuring machine compliance in compression. Load-displacement data is collected for the elastic compression of an aluminum cylinder of known properties. As shown in Figure (A2.1), the algebraic difference of the measured data and the calculated behavior of the test cylinder yields the machine compliance according to:

$$(\frac{dv}{dP})_{meas} = (\frac{dv}{dP})_m + (\frac{dv}{dP})_s \qquad \text{(A2.1)}$$

When the test cylinder is designed to yield plastically at 90% of the load cell capacity, then there is much less risk of damaging the load cell.

The Lazy-L tests were conducted on an Instron 1125 testing machine with a 20,000 pound capacity load cell. A test cylinder of 6061-T6 aluminum was designed for

use in measuring machine compliance. The diameter of the cylinder was chosen to assure yielding below the capacity of the load cell using the Von Mises yield criterion:

$$\sigma_Y = \{\frac{1}{2}[(\sigma_x - \sigma_y)^2 + (\sigma_y - \sigma_z)^2 + (\sigma_z - \sigma_x)^2]\}^{\frac{1}{2}} \qquad \text{(A2.2)}$$

For stress in the x-direction only, equation (A2.2) predicts yielding when $-\sigma_x$ is equal to the yield stress of the material; thus, for yielding at 90% of the maximum load cell capacity, cylinder sizing is governed by:

$$R^2 = \frac{0.9P_{\max}}{\pi Y} \qquad \text{(A2.3)}$$

For load cell capacity, P_{max}, of 20,000 pounds and yield stress, Y, of 40,000 psi, equation (A2.3) requires a radius, R, of 0.378 inches. The test cylinder used was a two inch length of 0.75 inch diameter stock.

Representative load-displacement data collected for this test specimen is shown in Figures (A2.2) and (A2.3). Note that the data acquisition system computes displacement as the product of crosshead speed and time, such that negative displacement increments during unloading appear as positive displacement increments and result in the triangular shape of the curve.

The slope of the measured data, $(dP/dv)_{meas}$, is 7558.5 lbs/0.5 mm or 383,875 lbs/in. For this load increment, test cylinder displacement is calculated using:

$$dv_s = \frac{LdP}{AE} \qquad \text{(A2.4)}$$

where dv_S is the change in specimen displacement, L is the specimen length, dP is the change in measured load, A is the area of the cylinder face and E is the Young's modulus

of the material which is 10e+06 psi for 6061-T6 aluminum. From equation (A2.4), dv_S corresponding to a 7558.5 pound load increment is 0.00342 inches; therefore, dv_m, equal to $(dv_{meas} - dv_S)$, is 0.01627 inches and $(dv/dP)_m$ is 2.15e-06 in/lb.

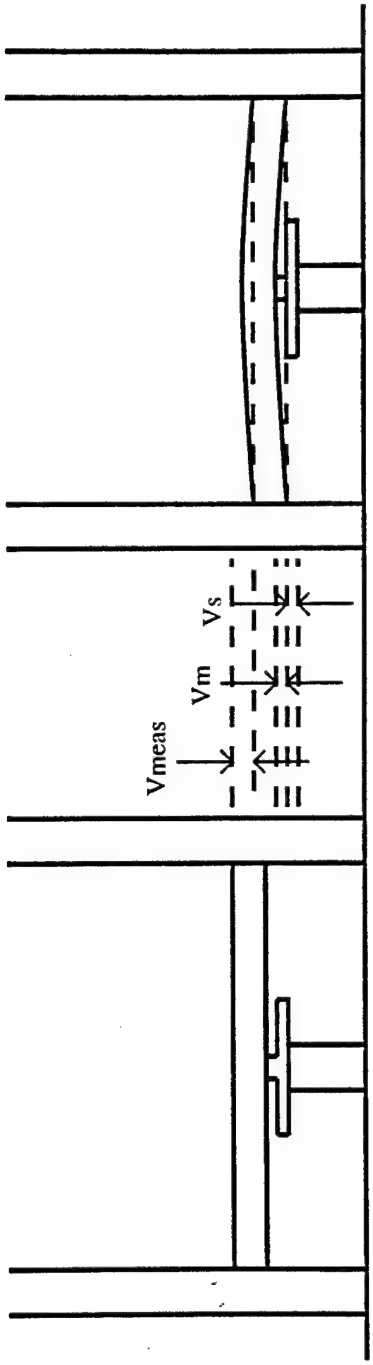

Figure A2.1: Machine, Specimen, and Measured Displacements

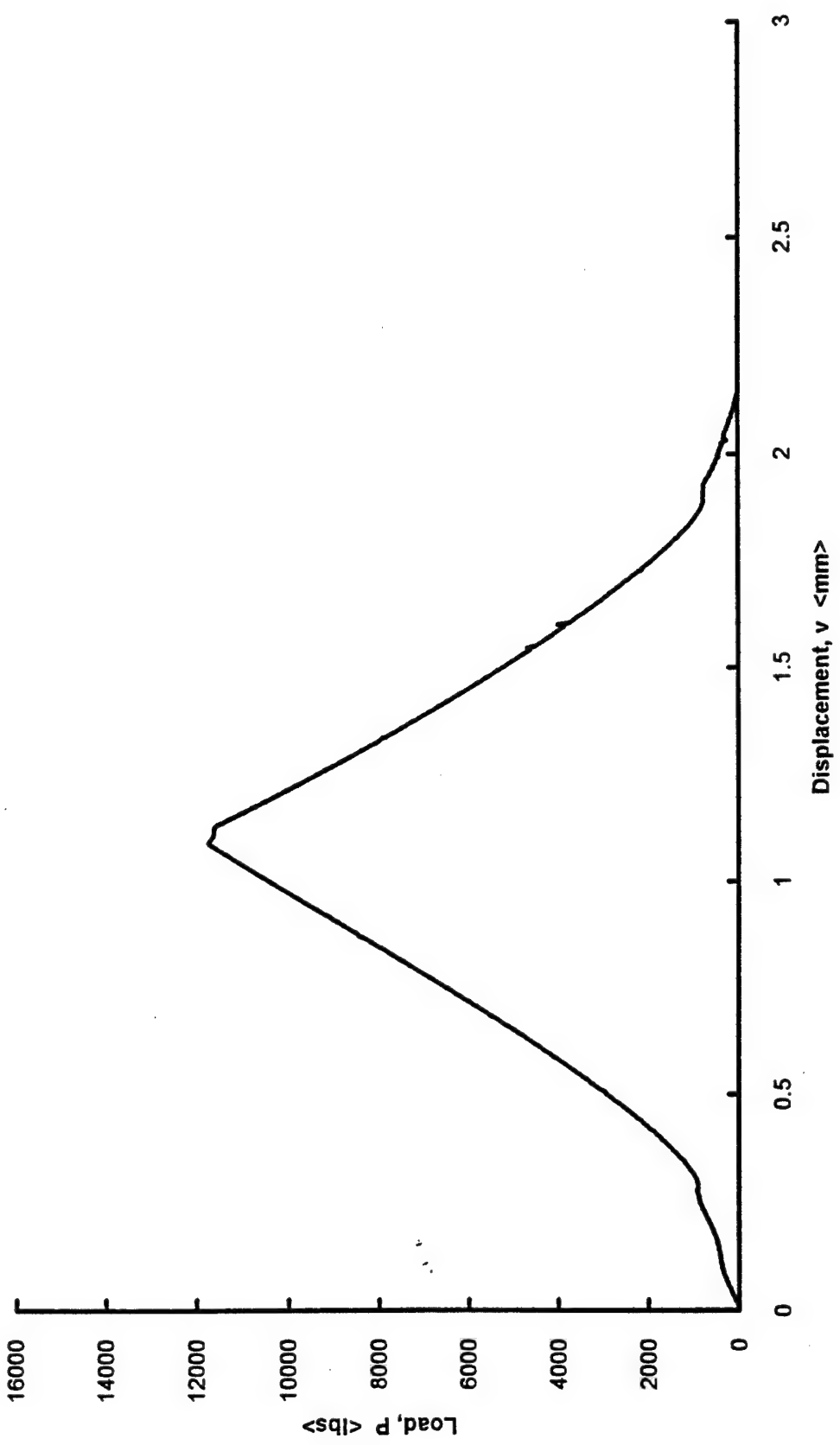

Figure A2.2: Load-Displacement Graph for 6061-T6 Aluminum Cylinder (1st)

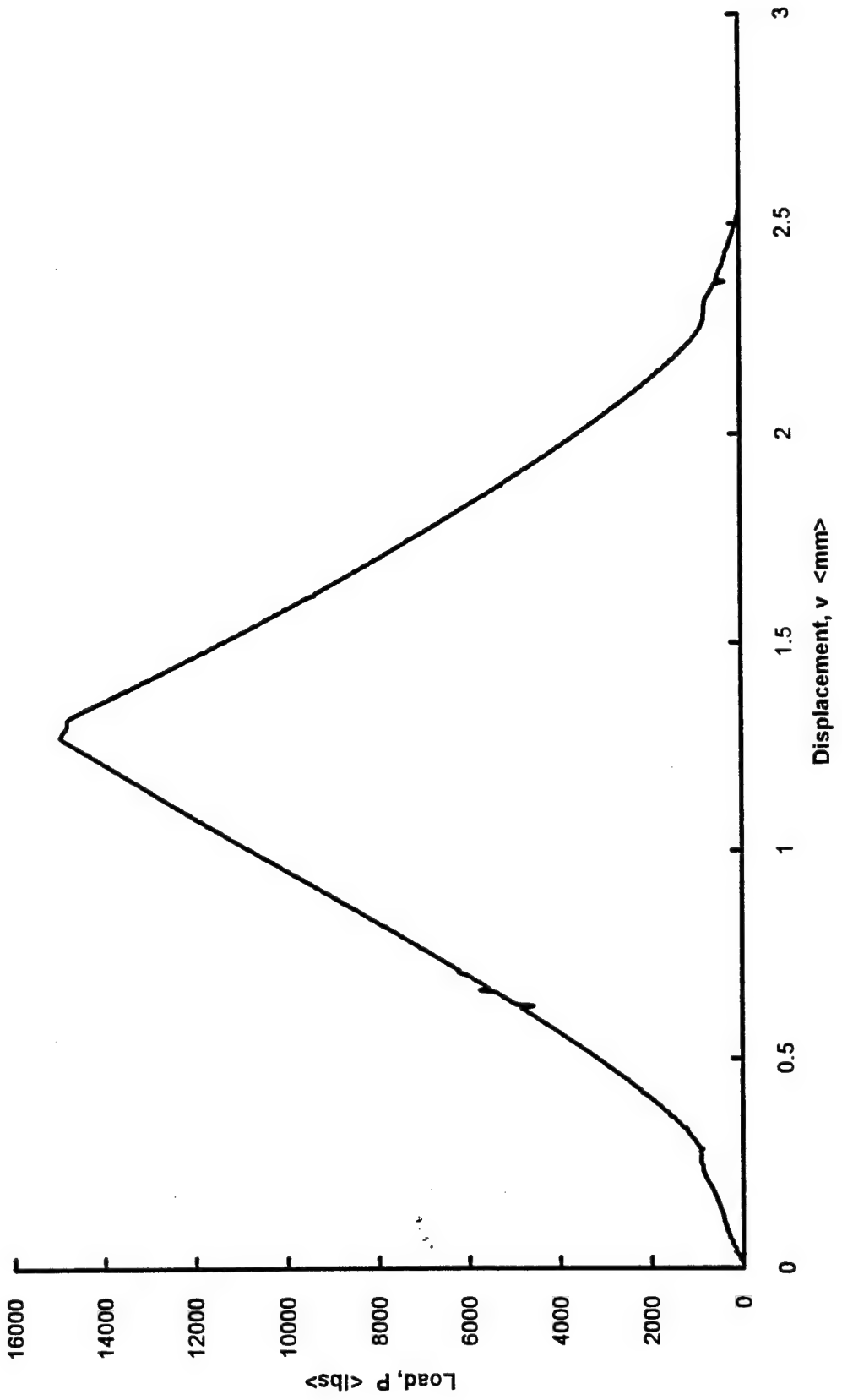

Figure A2.3: Load-Displacement Graph for 6061-T6 Aluminum Cylinder (2nd)

Appendix 3: Web and Fillet Shear Strength from Superficial Hardness

The shear strengths of the fillet and the web metal, k_f and k_w, are estimated from Rockwell superficial hardness readings taken within each region of the specimen. Although the correlations of hardness to tensile strength and tensile strength to shear strength are approximate, this method is the most convenient for a reasonable degree of accuracy. First, the test specimens are surface ground to a smooth finish. Water cooling is recommended to prevent surface hardening during specimen preparation. Next, the specimens are measured using the N Brale indenter on a Rockwell superficial hardness tester with 15 kilogram load.

Readings are taken at several locations within the base metal and weld metal. Readings are not taken within the heat affected zone for two reasons. First, the fillet shear strength of interest is that along the slip line. The slip lines for all three Lazy-L configurations occur in the weld metal. Second, the normalizing variable is a function of the shear strength of the web metal before welding.

Because the hardness reading is a measure of the plastic deformation of the material, readings must be spaced by least three diameters of the indenter from each other and from the edge of the specimen. Note that the first few reading are often inaccurate since the indenter must be well seated before testing; therefore, a calibration block is used until the readings are accurate.

Shear strength estimates from hardness data assume roughly uniform material properties in both the web metal and base metal; therefore, an average hardness reading is taken from a set of consistent measurements within each region of the specimen. The readings are converted to tensile strength using a hardness conversion chart. Table (A3.1) illustrates relevant portions of the Wilson hardness conversion chart for superficial hardness. All readings taken in the pilot Lazy-L experiments were below the 15N scale. Since the 45N scale represents three times the load of the 15N scale at the same

indentation, however, the measurements were read on the 45N scale and converted to one-third the linearly interpolated, corresponding tensile strength. The shear strength of the web, k_w, is taken as the tensile strength times $1/\sqrt{3}$ and the shear strength of the fillet, k_f, is taken as the tensile strength times 0.75 (Krumpen and Jordan, 1984) perhaps due to increased strain hardening in a confined region.

Table (A3.2) shows the hardness readings and corresponding tensile and shear strengths for the Lazy-L specimens tested.

Table A3.1: Wilson Rockwell Hardness Conversion Chart

Hardness Reading		Tensile Strength
15 N 15kg / N Brale	45 N 45 kg / N Brale	KSI
85.5	55.0	255
85.0	53.8	246
84.5	52.5	238
83.9	51.4	229
83.5	50.3	221
83.0	49.0	215
82.5	47.8	208
82.0	46.7	201
81.5	45.5	194
80.9	44.3	188
80.4	43.1	182
79.9	41.9	177
79.4	40.8	171
78.8	39.6	166
78.3	38.4	161
77.7	37.2	156
77.2	36.1	152
76.6	34.9	149
76.1	33.7	146
75.6	32.5	141
75.0	31.3	138
74.5	30.1	135
73.9	28.9	131
73.3	27.8	128
72.8	26.7	125
72.2	25.5	123
71.6	24.3	119
71.0	23.1	117
70.5	22.0	115
69.9	20.7	112
69.4	19.6	110

Table A3.2: Fillet and Web Metal Shear Strength from Rockwell Superficial Hardness

Specimen <by weld leg>	Hardness Reading Fillet <15 N>	Hardness Reading Web <15 N>	Tensile Strength Fillet <KSI>	Tensile Strength Web <KSI>	Shear Strength Fillet <KSI>	Shear Strength Web <KSI>	Shear Strength Fillet <lbs/mm^2>	Shear Strength Web <lbs/mm^2>
Single Fillet Bending								
6mm (1st)	41.4	23.9	58.09	39.44	43.57	22.77	67.53	35.29
6mm (2nd)	43.0	25.5	60.53	41.00	45.40	23.67	70.37	36.69
6mm (3rd)	37.0	25.0	51.76	40.44	38.82	23.35	60.17	36.19
9mm (1st)	41.8	22.0	58.82	38.33	44.12	22.13	68.38	34.30
9mm (2nd)	41.8	25.5	58.82	41.00	44.12	23.67	68.38	36.69
9mm (3rd)	43.0	24.7	60.53	40.11	45.40	23.16	70.37	35.89
Single Fillet Trans. Shear								
6mm (1st)	41.6	24.1	58.45	39.56	43.84	22.84	67.95	35.40
9mm (1st)	43.0	22.2	60.53	38.45	45.40	22.20	70.37	34.41
9mm (2nd)	40.8	24.7	57.00	40.11	42.75	23.16	66.26	35.89
Double Fillet Bending								
6mm (1st)	44.2	23.0	62.50	38.94	46.88	22.48	72.66	34.85
6mm (2nd)	42.3	25.3	59.56	40.78	44.67	23.54	69.24	36.49
9mm (1st)	39.3	23.5	54.92	39.22	41.19	22.64	63.84	35.10

Appendix 4: Moment-Rotational Displacement Graphs for Lazy-L Experiments

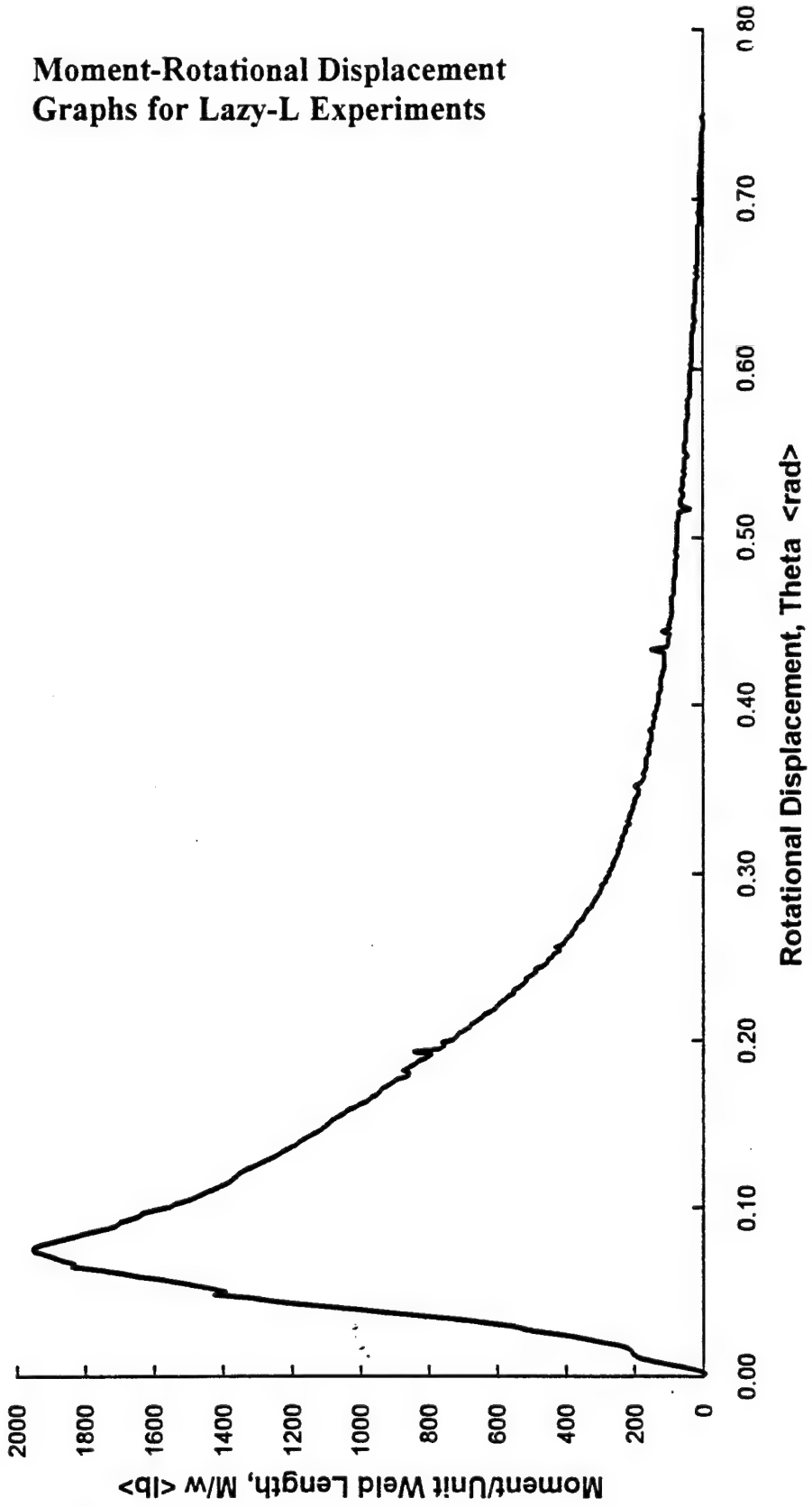

Figure A4.1 Moment per Unit Weld Length vs. Rotational Displacement for 6mm Fillet in Predominant Bending (1st)

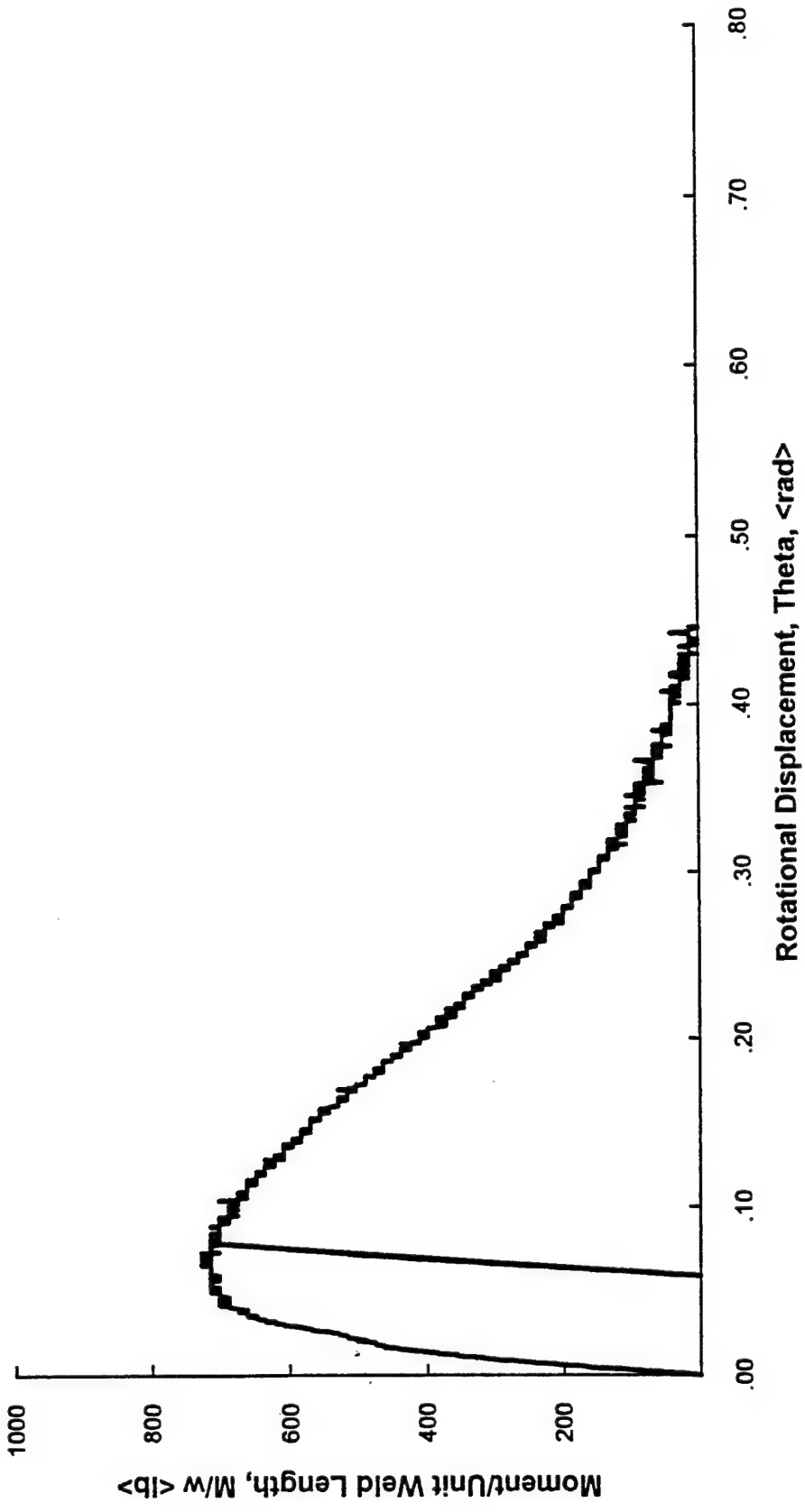

Figure A4.2 Moment per Unit Weld Length vs. Rotational Displacement for 6mm Fillet in Predominant Bending (2nd)

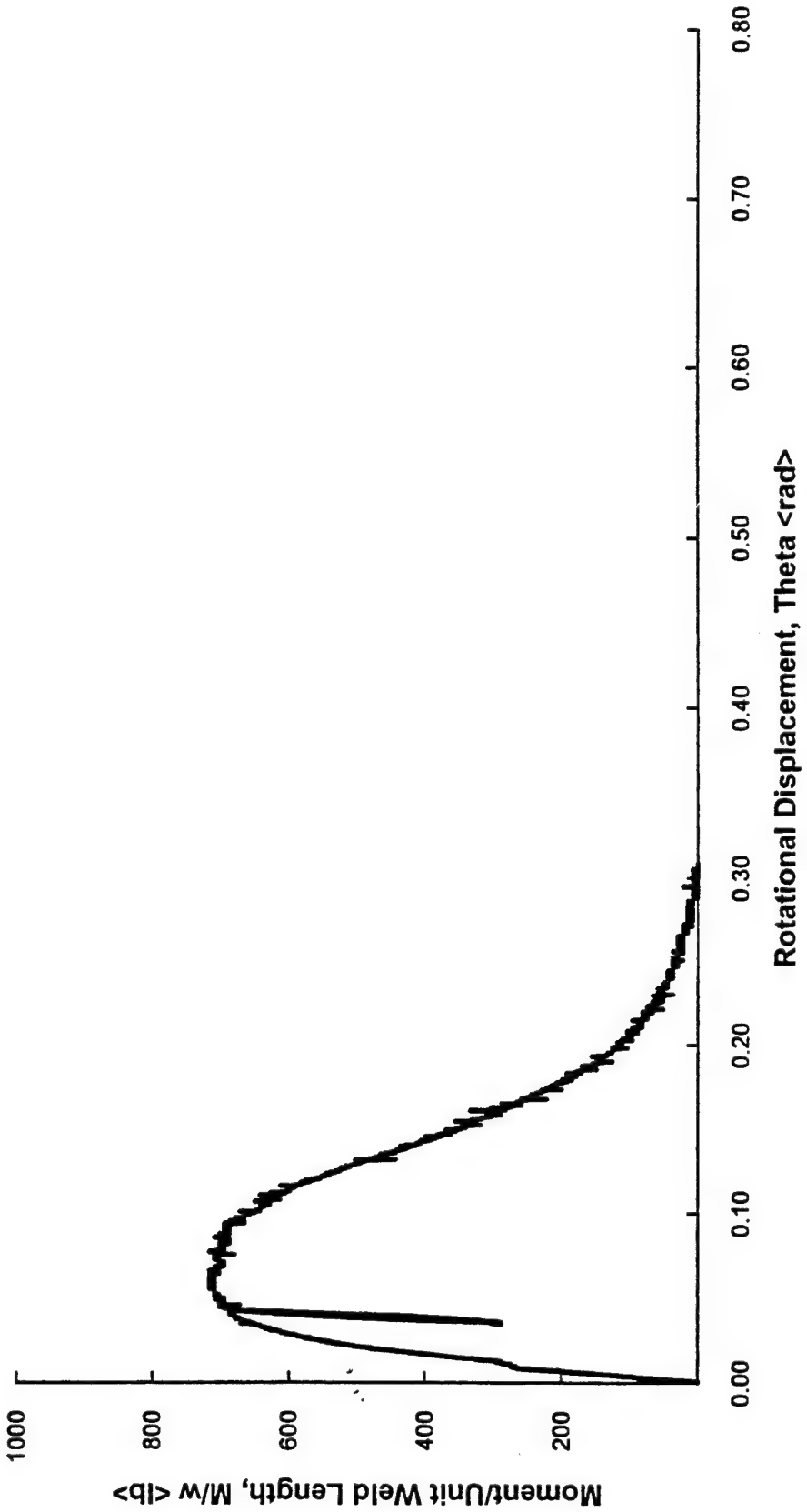

Figure A4.3 Moment per Unit Weld Length vs. Rotational Displacement for 6mm Fillet in Predominant Bending (3rd)

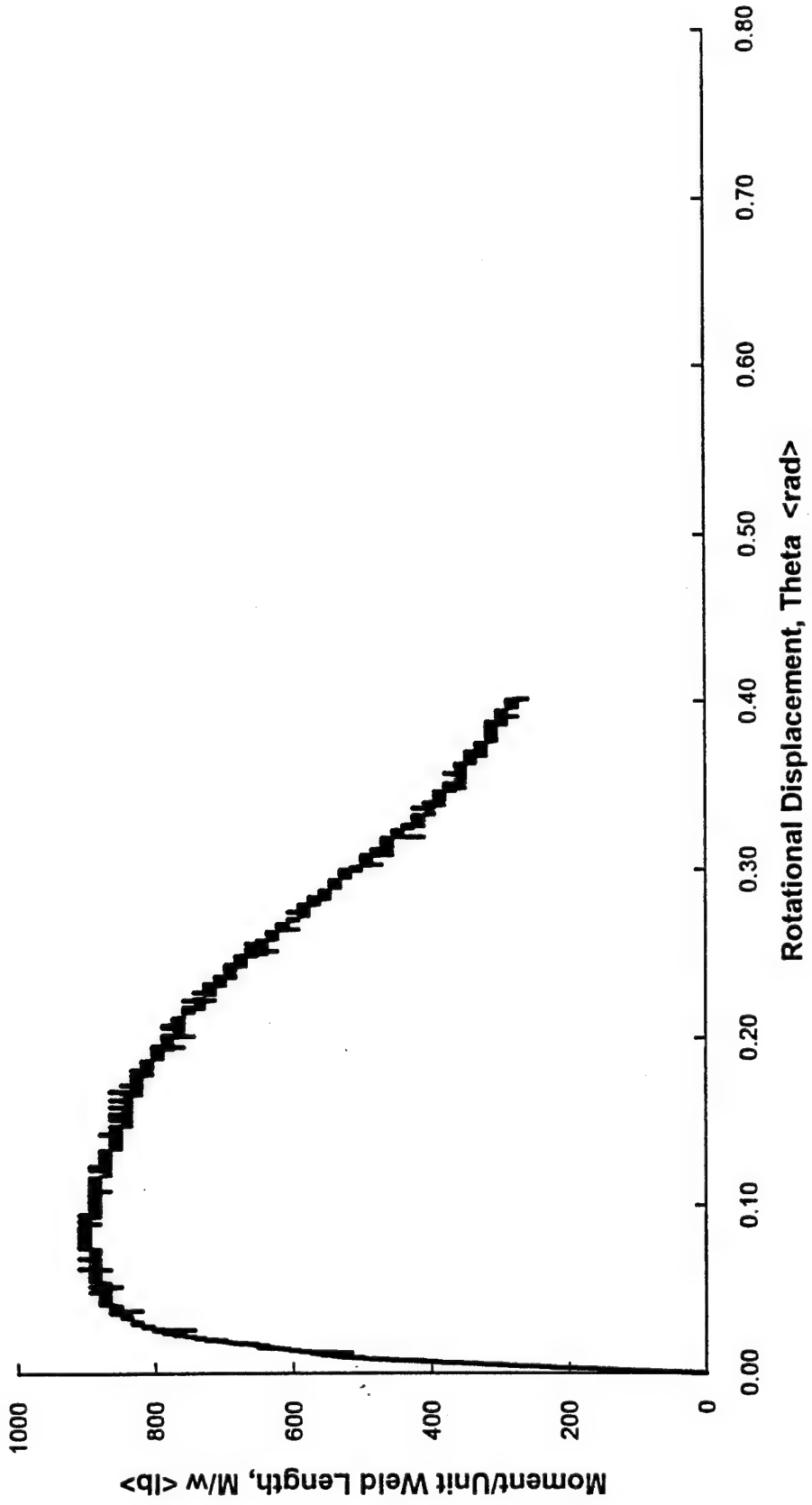

Figure A4.4 Moment per Unit Weld Length vs. Rotational Displacement for 9mm Fillet in Predominant Bending (1st)

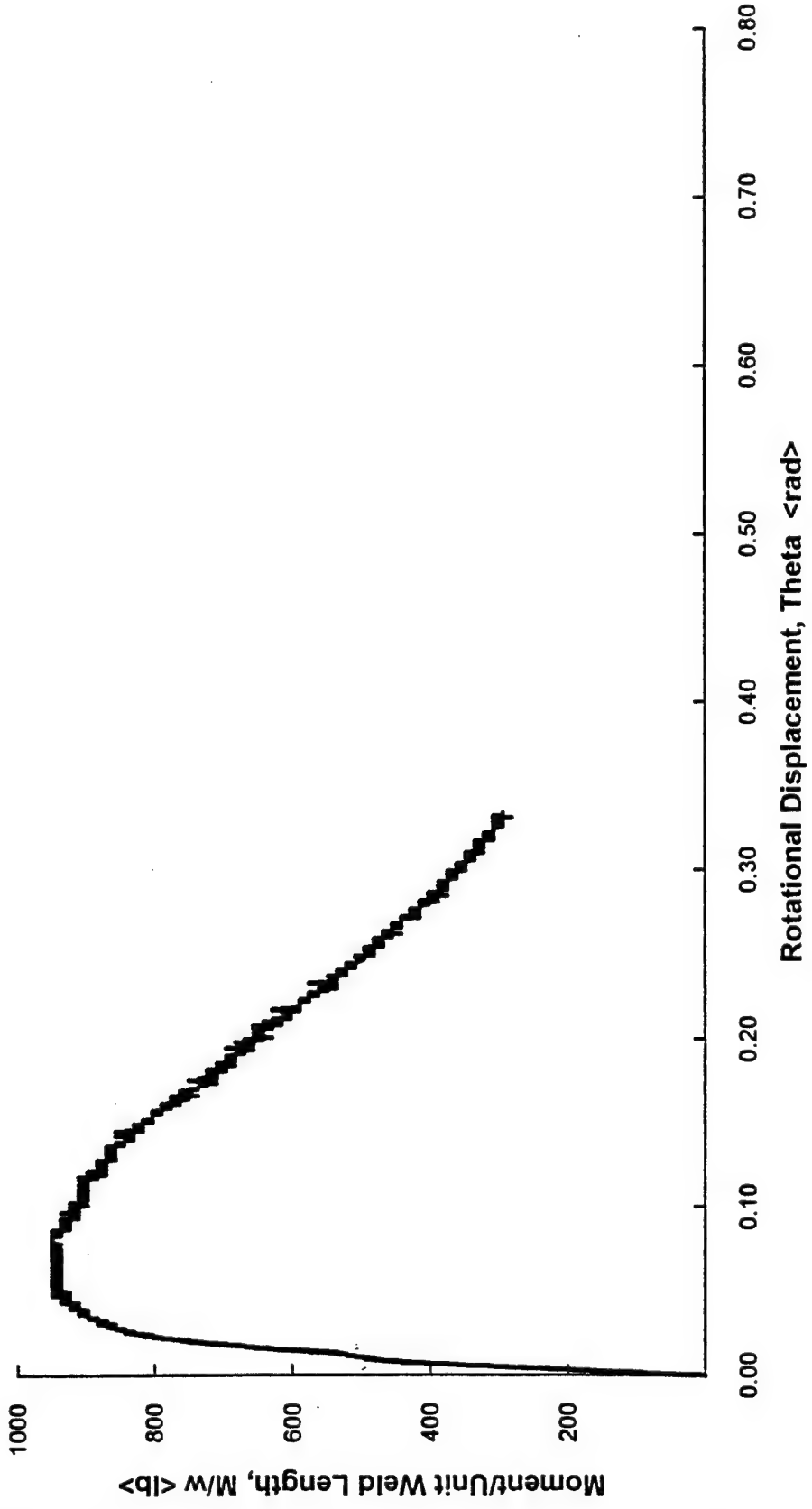

Figure A4.5 Moment per Unit Weld Length vs. Rotational Displacement for 9mm Fillet in Predominant Bending (2nd)

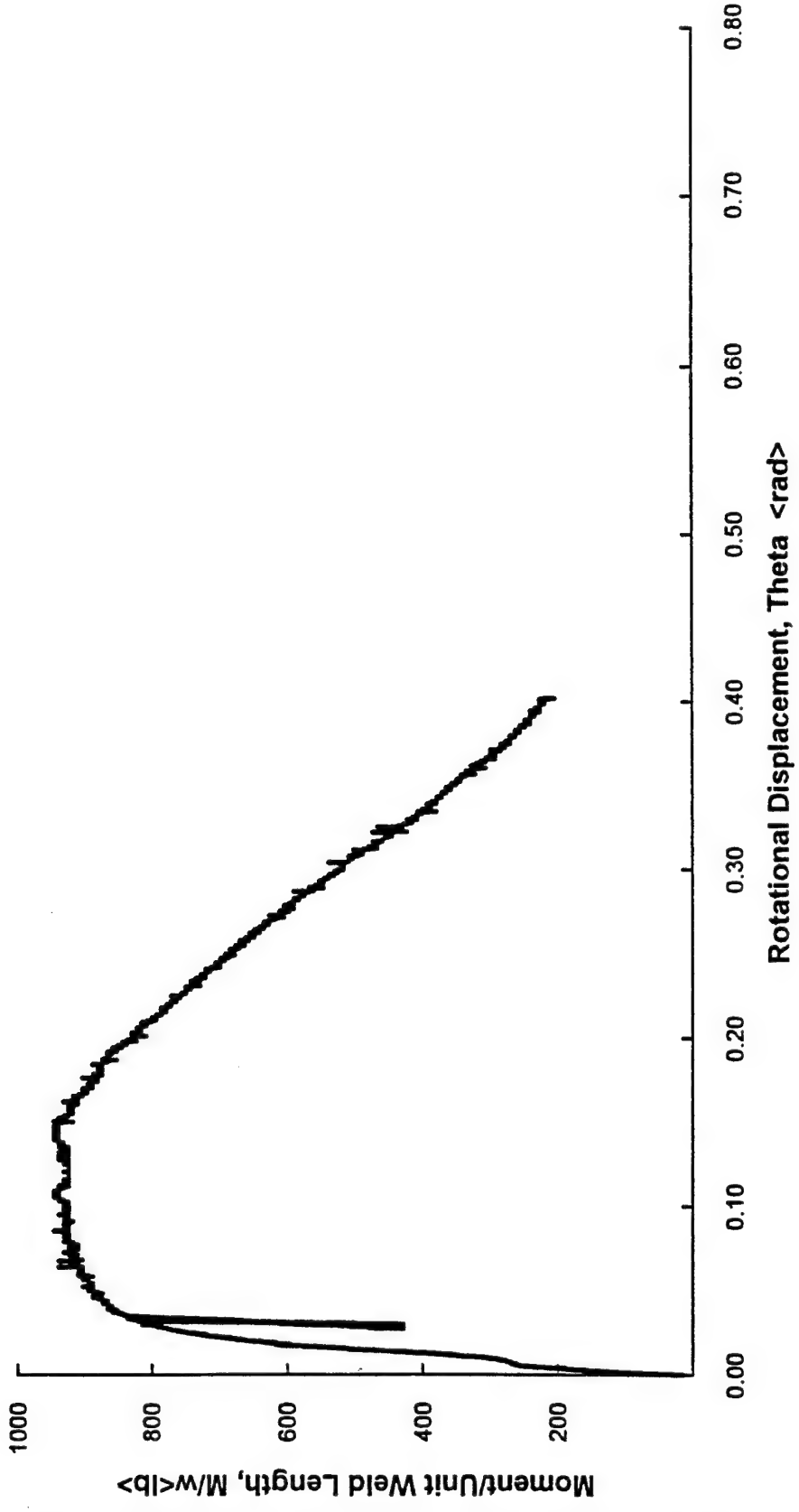

Figure A4.6 Moment per Unit Weld Length vs. Rotational Displacement for 9mm Fillet in Predominant Bending (3rd)

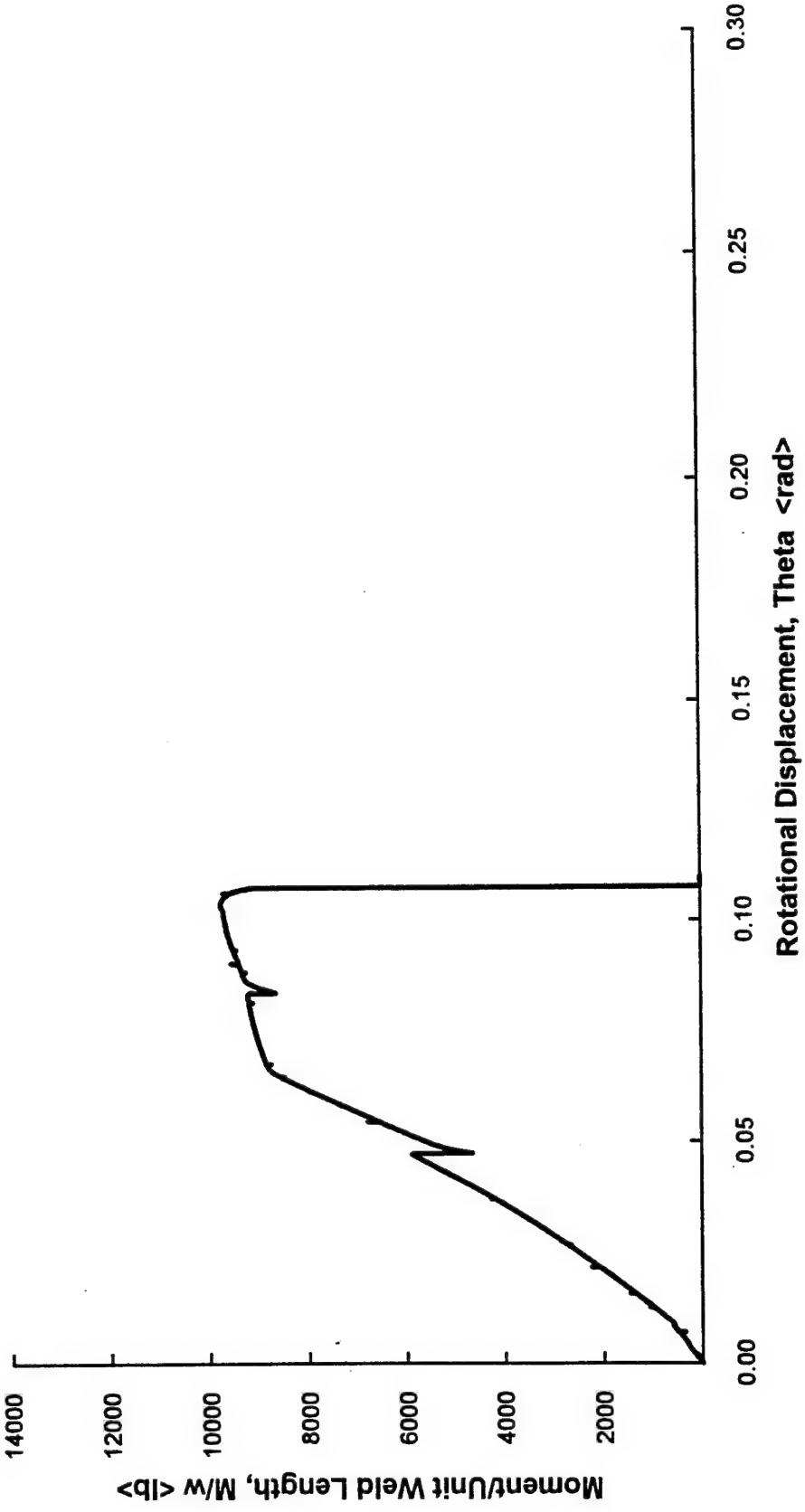

Figure A4.7 Moment per Unit Weld Length vs. Rotational Displacement for 6mm Fillet in Predominant Transverse Shear (1st)

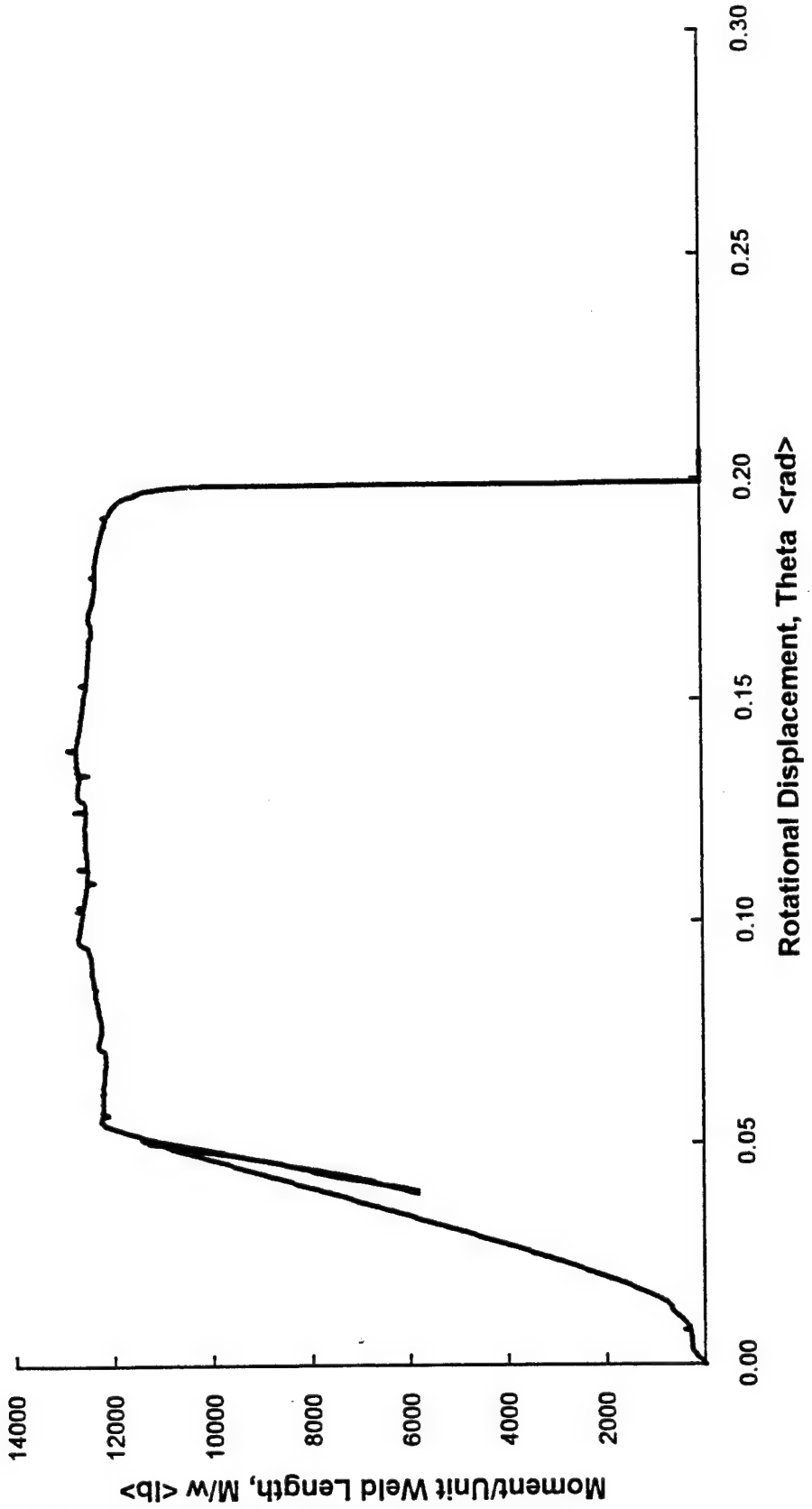

Figure A4.8 Moment per Unit Weld Length vs. Rotational Displacement for 9mm Fillet in Predominant Transverse Shear (1st)

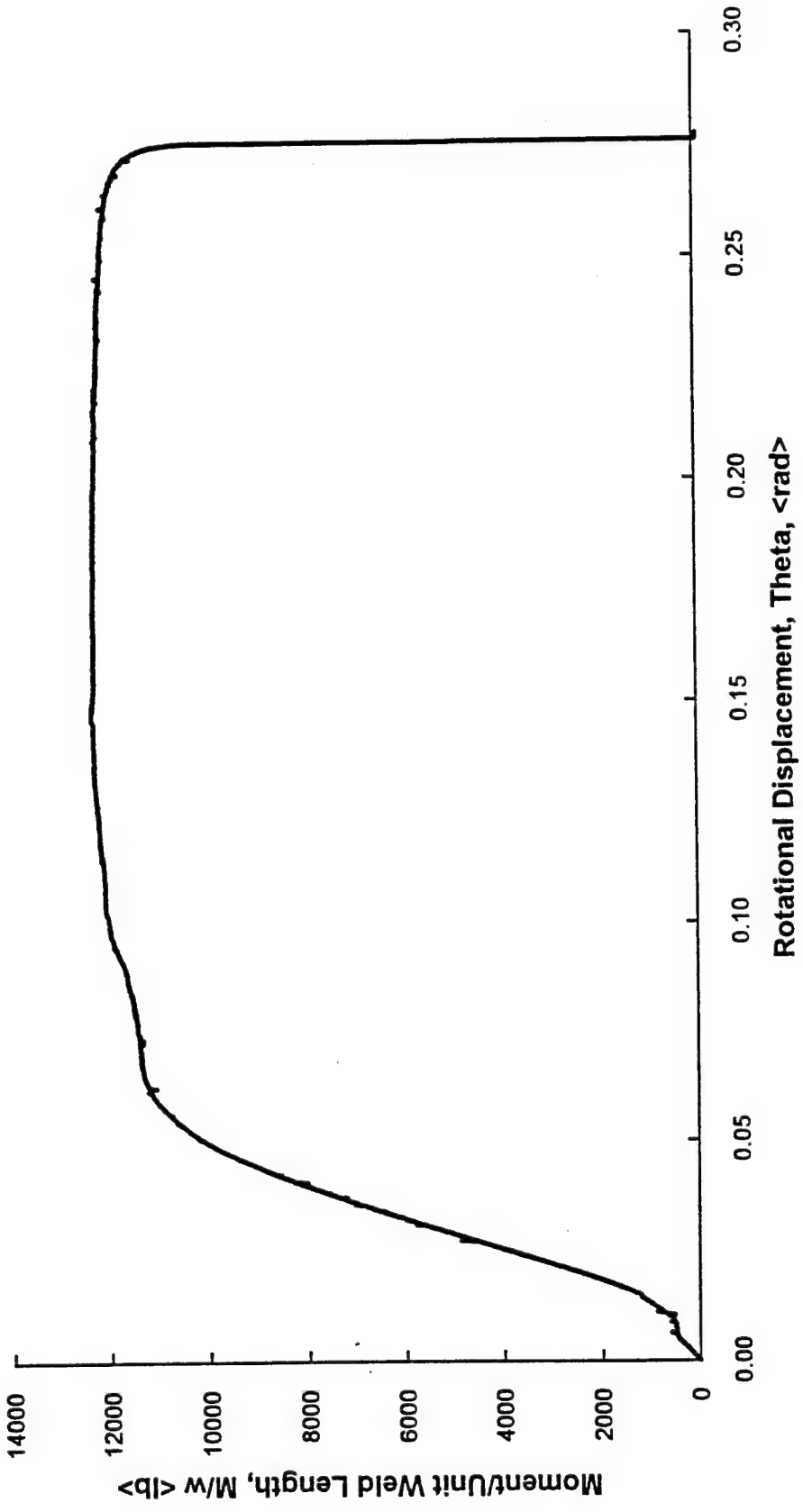

Figure A4.9 Moment per Unit Weld Length vs. Rotational Displacement for 9mm Fillet in Predominant Transverse Shear (2nd)

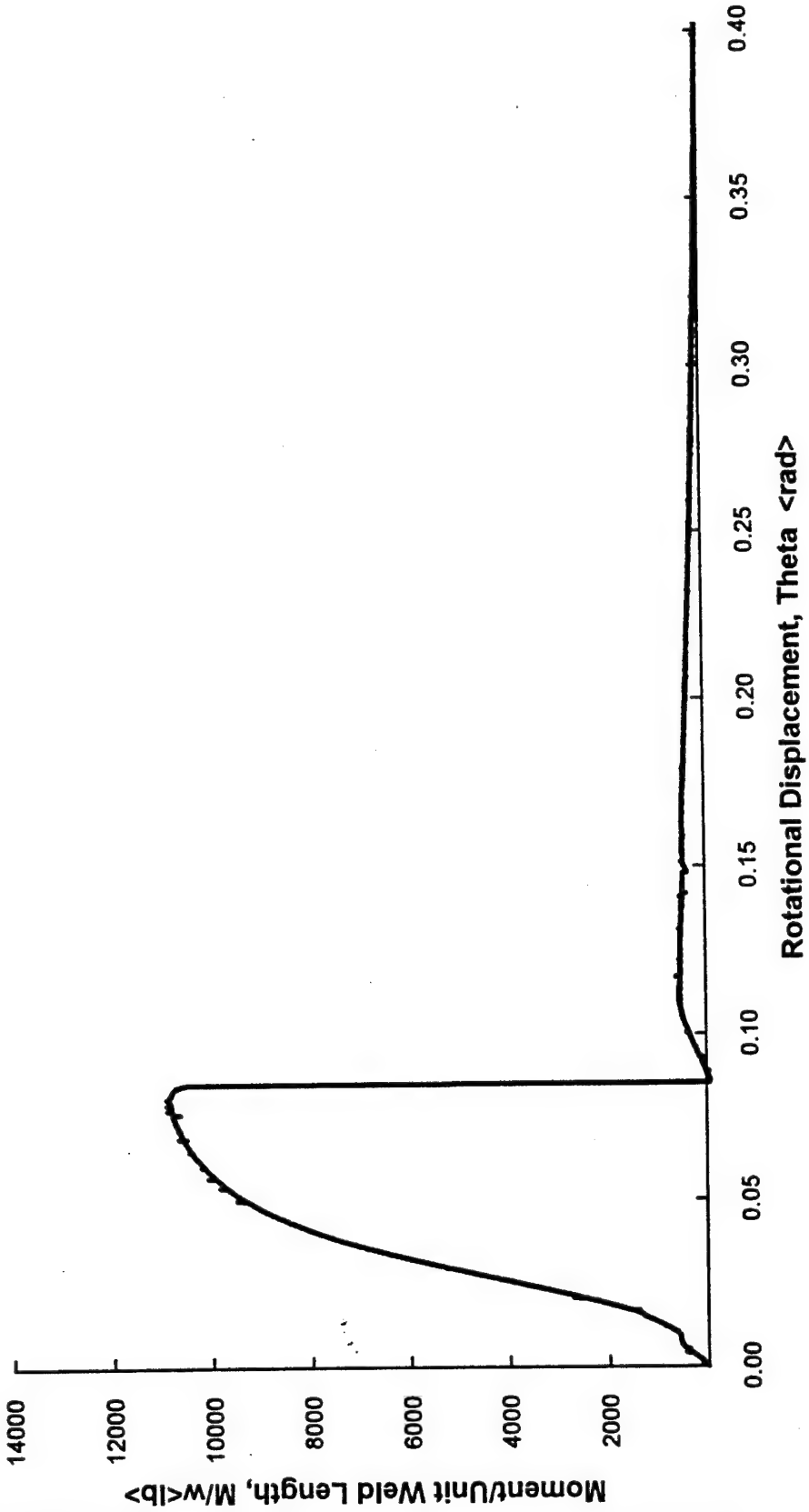

Figure A4.10 Moment per Unit Weld Length vs. Rotational Displacement for Double 6mm Fillet in Predominant Bending (1st)

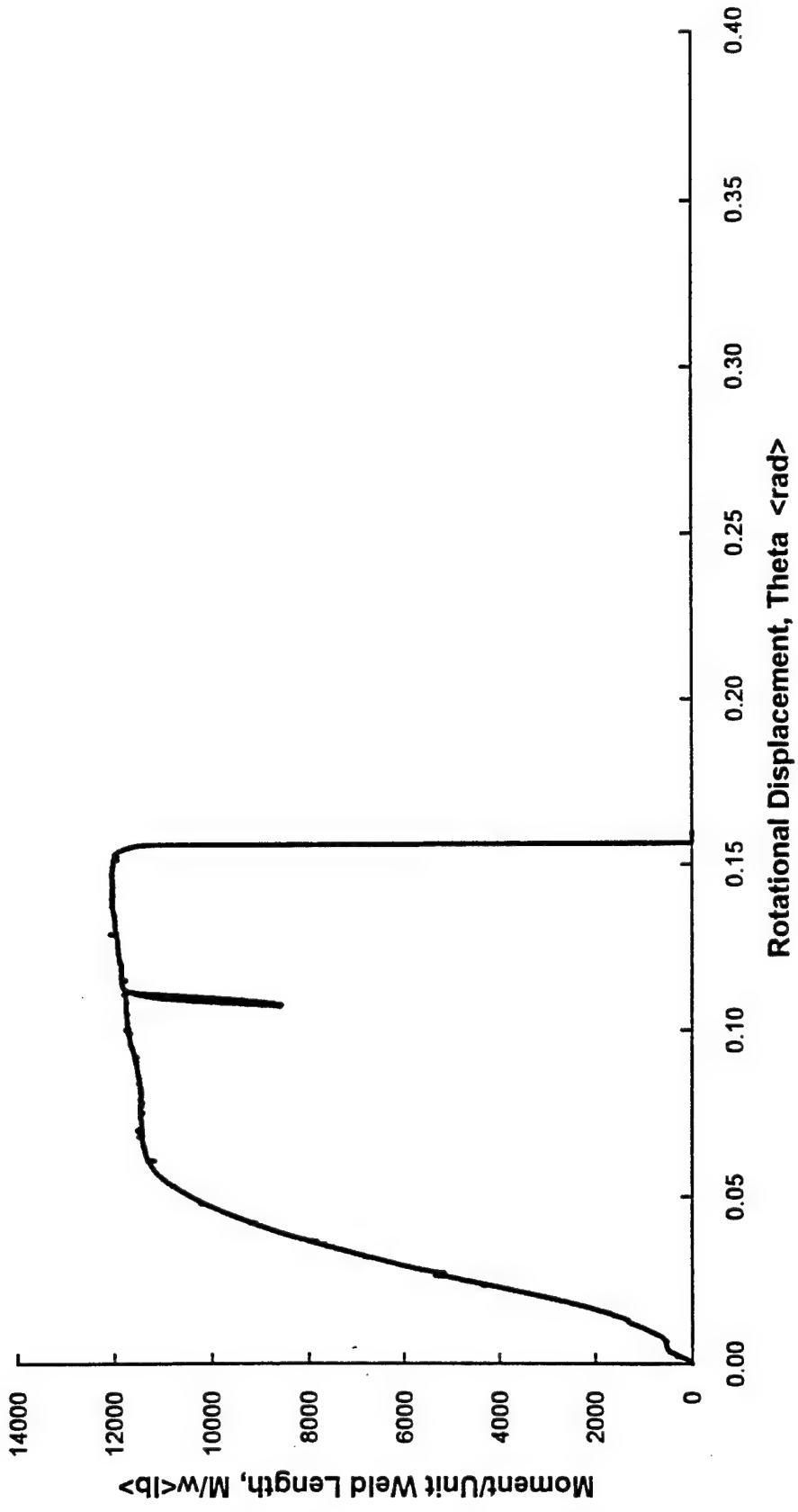

Figure A4.11 Moment per Unit Weld Length vs. Rotational Displacement for Double 6mm Fillet in Predominant Bending (2nd)

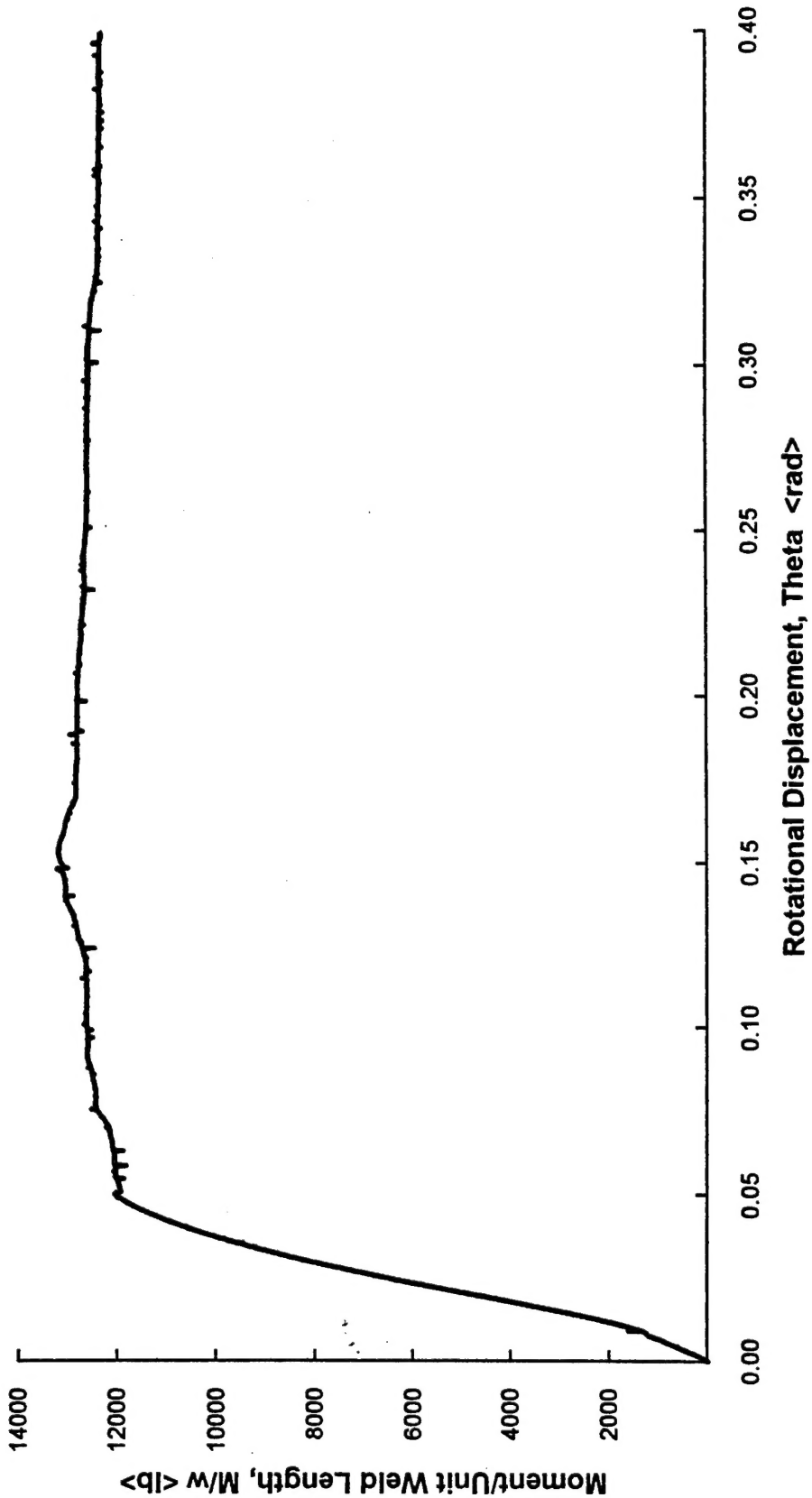

Figure A4.12 Moment per Unit Weld Length vs. Rotational Displacement for Double 9mm Fillet in Predominant Bending (1st)

Appendix 5: Test Machine Calibration and Data Acquisition

The Lazy-L test experiments were conducted on an Instron 1125 universal testing machine in Mechanical Behavior of Material Lab at the M.I.T. Department of Mechanical Engineering. The following is provided as a reference for future tests at this and similar facilities.

A5.1 Machine Setup

After a fifteen minute warm-up, the Instron 1125 with 20,000 lb. load cell must be zeroed and balanced. Switch the load shunt resistance to OFF and select polarity on the load cell amplifier for compression. With the test grips in place, hold the zero button on the load cell amplifier and adjust the adjacent dial until the voltmeter reads 0.00. Release the zero button and adjust the load cell amplifier balance dials (coarse, medium, fine) until the voltmeter again reads 0.00. This procedure sets the reference of the bridge and compensates for the static load of the test fixtures.

Next, the load must be calibrated. The Instron 1125 is equipped with shunt resistors which simulate a range of loads. Table (A5.1) illustrates the equivalent load of the available shunt resistors for the 20,000 lb. load cell. The voltmeter range is 0-10 Volts; therefore a convenient scale is 1V = 2000 lb. Notice from Table (A5.1) that the 100,000 Ohms resistor simulates a load of 2916 lb. in compression. The desired voltmeter reading for this resistor is found as:

$$\frac{2916lb.}{2000lb./Volt} = 1.46V \qquad \text{(A5.1)}$$

With the 100K shunt resistor selected, adjust the full scale load dial to a low setting for high resolution of the load voltmeter scaling. Adjust the calibration dial until the voltmeter reads 1.46 but do not press the adjacent calibration button. Return the shunt resistance to OFF and check the balance. Adjust the balance until the voltmeter reads 0.00. Compute the expected voltmeter reading for adjacent shunt resistors and check that the scaling is tuned at several different loads. When the scaling is well tuned, the voltmeter reading does not change when the full scale load dial is returned to 20,000 lb.

A5.2 Data Acquisition

Details of the data acquisition software are omitted. Note, however, that Labtech Notebook treats both the load and displacement as calculated variables. Notebook samples the voltmeter output at a rate selected by the user to provide good resolution at the selected crosshead speed. The load is computed as the product of the voltmeter readings and a factor entered by the user. For the example given, this factor is 2000. Displacement is computed as the product of elapsed time and the crosshead speed entered by the user. Since the displacement in the Lazy-L tests are small, a convenient displacement scale is millimeters. For crosshead speed selected as 0.05 inches/minute, the appropriate factor is 0.2117 mm/s. Test duration is a function of the crosshead speed and specimen size. Test times for the pilot experiment at the speed indicated averaged roughly 300 seconds.

Table A1.5: 20,000 Pound Load Cell Calibration

Instron 1125, Serial No. 307

Calibration June 19, 1982 by W.T. Carter

Shunt Resistance	Load			
	Tension		Compression	
(Ohms)	(lb)	(N)	(lb)	(N)
10M	26.5	118	32.0	142
5M	56.0	249	61.5	274
2M	143.0	636	143.0	658
1M	288.5	1283	293.0	1303
500K	581.0	2584	584.0	2598
200K	1452.0	6458	1450.0	6450
100K	2930.0	12988	2916.0	12965
50K	5830.0	25931	5810.0	25842
20K	14460.0	64318	14400.0	64051
10K	---	---	---	---